Volatile opinions and optimal control of vaccine awareness campaigns: chaotic behaviour of the forward-backward sweep algorithm vs. heuristic direct optimization

Rossella Della Marca[a,*], Alberto d'Onofrio[b,c,1,*]

[a] Department of Mathematical, Physical and Computer Sciences, University of Parma, Parco Area delle Scienze 53/A, Parma 43124, Italy
[b] Department of Mathematics and Statistics, University of Strathclyde, 26 Richmond Street, Glasgow G1 1XH, United Kingdom
[c] International Prevention Research Institute, 95 cours Lafayette, Lyon 69006, France

A B S T R A C T

In modern societies the main sources of information are Internet-based social networks. Thus, the opinion of citizens on key topics, such as vaccines, is very volatile. Here, we explore the impact of volatility on the modelling of public response to vaccine awareness campaigns for favouring vaccine uptake. We apply a quasi-steady-state approximation to the model of spread and control of Susceptible-Infected-Removed diseases proposed in (d'Onofrio et al., PLoS One, 2012). This allows us to infer and analyze a new behavioural epidemiology model that is nonlinear in the control. Then, we investigate the efficient design of vaccine awareness campaigns by adopting optimal control theory. The resulting problem has important issues: (i) the integrand of its objective functional is non-convex; (ii) the application of forward-backward sweep (FBS) and gradient descent algorithms in some key cases does not work; (iii) analytical approaches provide continuous solutions that cannot rigorously be implemented since Public Health interventions cannot be fully flexible. Thus, on the one hand, we resort to direct optimization of the objective functional via heuristic stochastic optimization, in particular via particle swarm optimization and differential evolution algorithms. On the other hand, we investigate the non-convergence of the FBS algorithm with tools of the statistical theory of nonlinear chaotic time-series. Finally, since the direct optimization algorithms are stochastic, we provide a statistical assessment of the obtained solutions.

1. Introduction

A major challenge for global Public Health (PH) is the spread of hesitancy and refusal of vaccines to prevent childhood diseases. This is due to the phenomenon of 'pseudo-rational' exemption to vaccination: parents overweight real and imaginary side effects of vaccines and underweight real risks due to the target infectious diseases. To mitigate the impact of this challenge, the Public Health Systems (PHSs) may counteract by means of public campaigns to favour vaccine uptake.

* Corresponding author.
E-mail addresses: rossella.dellamarca@unipr.it (R. Della Marca), alberto.donofrio@i-pri.org, adonofrio1967@gmail.com (A. d'Onofrio).
[1] Co-Corresponding Author: Dr. Alberto d'Onofrio is no more affiliated to International Prevention Research Institute.

These scenarios make it increasingly important a new approach to modelling the spread and control of infectious diseases, by including in the modelling the description of human decision making. This led to the birth of a new scientific discipline: the behavioural epidemiology of infectious diseases [42,62]. In particular, the complex dynamics of vaccine decision has been modelled as an imitation game [4,17] or, equivalently, as an infection of ideas process [62]. The approach introduced in [4,17] was suitably modified by d'Onofrio et al. [18] in order to take into the account the actions enacted by PHS to favour vaccination.

In papers [4,17,18] the analytical and numerical investigations were focused on scenarios where citizens slowly change their opinion. This assumption, however, in the age of social media is increasingly questionable. Nowadays, the opinion form is based on information and rumors collected and exchanged on Internet-based social media such as Facebook, Twitter, Instagram, TikTok, etc., and, at the micro-scale of small chat groups, WhatsApp, Snapchat, Telegram and Facebook Messenger. This impressive *exponential growth in public opinion channels* [34] makes the opinion of population much more volatile than in the past on many sensitive subjects [1], including politics [1,33] and vaccines [8,47]. Such a radical change of scenario must be taken into the account in the models of behavioural epidemiology of infectious diseases.

We are here particularly interested in the optimal design of the awareness campaign in the current context of extremely volatile opinion among the population targeted by these campaigns by applying optimal control (OC) theory.

OC theory [21,36,53] is a classical tool applied in mathematical epidemiology of infectious diseases [2,3,5,6,38,39,54,55]. However, the adoption of an optimal control strategy, given an health economy objective and appropriate constraints, posits some remarkable problems. The first is common to a number of other problems in numerical analysis: the chosen numerical algorithms could lack convergence due to stiffness of the mathematical model or to complex chaotic behaviours induced by the recursive nature of the adopted algorithms. Sensitivity to initial conditions could make impossible to numerically solve a problem. The second is that the solution of the optimal control problem via the minimum principle by Pontryagin is a continuous function of time which requires a continuous adaptation of the PH intervention. Unfortunately, in most case a PHS is not endowed for practical reasons such a large degree of flexibility. The third problem is that, once obtained the optimal solution for the control (we denote it $\gamma(t)$), one has no indication of the degree of robustness of this solution. Due to the above-mentioned low degree of flexibility of the PHS action, it would be desirable to have an idea of how much a given OC solution is flexible to deviations. The fourth problem is also extremely relevant: it may happen that for the OC problem in study the requirements of classical existence theorems are not satisfied. One cannot say to PH officers that the problem cannot be investigated for lack of appropriate theorems.

The first problem was first faced in behavioural epidemiology by Buonomo et al. [12], whose solution led to consider, in part, the second one. On the contrary, the other two are specific to this work. Namely, in [12] the lack of convergence of some well-known OC algorithms aimed at the solution of the Pontryagin differential-algebraic constrained system [50], led the authors to consider the application of a direct optimization strategy. It was adopted the oldest algorithm of stochastic heuristic optimization, the simulated annealing [7]. This led to consider OC strategies that are piecewise-constant. This was needed for numerical analysis but was in the same time a first contribute to finding realistic OC strategies more adapt to the reality of not so flexible PH interventions.

We propose here some important novelties with respect to the paper [12]. First, we adopt two more recent and robust heuristic optimization algorithms [7]: the particle swarm optimization [7,35] and the differential evolution [7,52,57]. Note that we do not adopt these two well-known methods for comparing their performances: we choose them in order to have a double check of the results and of the robustness of the optimal control. Indeed, the direct optimization results obtained by means of two different algorithms allow us to better evaluate the robustness of the OC solution to temporary perturbations of large amplitude. Second, here we perform an analysis of the time-series of the economic objective generated by the OC algorithm in case of non-convergence. As far as the degree of flexibility of the vaccine awareness campaigns is concerned, we propose a more advanced analysis with respect to [12]. Indeed, we consider three strategies of intervention: with 3-months changes, with annual changes and with biennial changes.

Concerning the last problem, OC problem in study is characterized by an objective functional whose integrand is non-convex w.r.t. $\gamma(t)$. Moreover, at variance with many studies, in the proposed model the dependence on the control is non-linear.

The paper is organized as follows. In Section 2, we briefly present a general family of vaccination models following imitation game dynamics. The current scenario of rapid opinion switching is addressed in Section 3, where the new model is derived and its open-loop control via vaccine awareness campaigns is discussed. Then, we focus on the application of OC theory: in Section 4 the objective functional is defined and in Section 5 the necessary conditions of optimality are derived via the Pontryagin minimum principle. The OC problem parametrization and simulation scenarios are presented in Section 6. Then, we provide the numerical optimal solutions via some indirect (Section 7) and direct (Section 8) optimization methods. Since the latter are stochastic processes, a statistical assessment of the corresponding solutions is performed in Section 9. In Section 10, we apply the methods of nonlinear time-series theory to investigate the non-convergence of the indirect methods in some key cases. Finally, concluding remarks and future perspectives are given in Section 11. The paper is complemented by the Appendices A and B and a file of Supplementary Materials.

2. Background

Let us consider the Susceptible-Infected-Removed (SIR)-like model describing the dynamics of a vaccine-preventable childhood disease under voluntary vaccination choices introduced in [17,18]:

$$\begin{aligned} \dot{S} &= \mu(1-p(t)) - \beta SI - \mu S, \\ \dot{I} &= \beta SI - (\nu+\mu)I, \end{aligned} \tag{1}$$

where S and I denote the fraction of susceptible and infectious individuals w.r.t. the total population at time t, respectively; the time-dependent variable p models the vaccine uptake of newborns. The other parameters are positive constants: (i) birth and mortality rates are equal to a value μ (implying a stationary population); (ii) β is the transmission rate; (iii) ν is the recovery rate.

To model the impact of human responses to both the spread of the disease and vaccine adverse events on the dynamics of vaccine propensity p, we follow [4,17,18] and assume that there exist two interacting vaccine-related strategies among the (interacting) individuals: 'pro-vaccine' and 'anti-vaccine'. We denote by p and $A = 1 - p$ the fractions of the two above groups at time t.

The dynamics of p follows an imitation game dynamics that could be inferred by employing the concept of payoff [4,17]. However, many evolutionary game models belong to the class of 'urn' models [22], a wide family that includes chemical kinetics models as well as other models based on the mass action principle, such as the non-behavioural models of classical mathematical epidemiology. This statistical physics-oriented approach [9,62] allows a mechanistic inference of the dynamics of p that is much clearer than the classical economics-oriented approach based on payoffs. The basic idea is that the dynamics of p and A are ruled by a 'double contagion' of ideas between the two involved groups. This approach yields the following family of models:

$$\begin{aligned} \dot{p} &= k\theta(I)pA - k\alpha(M_{se})Ap, \\ \dot{A} &= -k\theta(I)pA + k\alpha(M_{se})Ap, \end{aligned}$$

where: (i) the 'force of infection' concerning the switch from the strategy 'no-vaccinator' to the strategy 'vaccinator' is $k\theta(I)p$, where $\theta(I)$ is an increasing function of prevalence of the disease; (ii) the 'force of infection' concerning the switch from the strategy 'vaccinator' to the strategy 'no-vaccinator' is $k\alpha(M_{se})A$ where $M_{se}(t)$ is an information variable on the extent of vaccine-related side effects; (iii) the parameter k, although not strictly necessary, is a time scale tuning parameter. Its role here is similar to the role of the parameter k in the Glauber model of the mean-field kinetic of phase transitions of the Ising model [27]: it characterizes the time scale of the velocity of opinion switching for the parents population.

The action of the PHS to favor the vaccine uptake is simply modelled as an additional switch from the strategy 'no vaccine' to the strategy 'vaccine'. This yields the model [62]

$$\begin{aligned} \dot{p} &= k\theta(I)pA - k\alpha(M_{se})Ap + k\gamma(t)A, \\ \dot{A} &= -k\theta(I)pA + k\alpha(M_{se})Ap - k\gamma(t)A. \end{aligned}$$

The function $k\gamma(t)$ represents the rate of switching from the strategy 'no vaccine' to the strategy 'vaccine' induced by the campaigns enacted by the Public Health System to increase the vaccine propensity. Taking into the account that $A = 1 - p$ yields the following model:

$$\dot{p} = kp(1-p)(\theta(I) - \alpha(M_{se})) + k\gamma(t)(1-p),$$

originally proposed by d'Onofrio et al. [18] by an economy-oriented game-theoretic approach. In the following we will focus on the case of linear $\alpha(M_{se})$, with M_{se} proportional to the vaccine uptake of newborns p, yielding (with slight abuse of notation) $\alpha(M_{se}) = \alpha p$. Hence, the equation for p reads

$$\dot{p} = kp(1-p)(\theta(I) - \alpha p) + k\gamma(t)(1-p). \tag{2}$$

In case of constant $\gamma(t) = \gamma = const.$ studied in [18], it was shown that public intervention has a stabilising role to reduce the strength of imitation-induced oscillations, and if $\gamma > \alpha p_c^2$ (with p_c given in (7)), to allow disease elimination by making the disease-free equilibrium where everyone is vaccinated globally attractive. The cases of periodic $\gamma(t)$ (corresponding to the alternate work-holidays terms) and of periodic contact rate were investigated, respectively, in [10] and in [9].

3. Modelling the current scenario of volatile opinions

To model the current scenario of volatile opinion switching, we assume that the imitation speed, tuned by the parameter k, is very rapid: $k \gg 1$. Thus, a *quasi-steady-state approximation* [40] for p can be used in (2), which yields:

$$p(1-p)(\theta(I) - \alpha p) + \gamma(t)(1-p) = \frac{\dot{p}}{k} \approx 0.$$

As a consequence, in the limit $k \to +\infty$, p is the solution of the following algebraic equation:

$$0 = (1-p)(\gamma(t) + \theta(I)p - \alpha p^2) \tag{3}$$

to be solved under the constraint:

$$0 \leq p \leq 1. \tag{4}$$

Eq. (3) with condition (4) has two solutions: $p = 1$, and the unique positive solution of

$$\gamma(t) + \theta(I)p - \alpha p^2 = 0.$$

Summarizing, p tends to

$$p = \zeta(I, \gamma(t)) = \min\left(1, \frac{\theta(I) + \sqrt{\theta^2(I) + 4\alpha\gamma(t)}}{2\alpha}\right) \tag{5}$$

because it is stable, at variance of $p = 1$ which is unstable. In other words: (i) if $p = \zeta$, then $\dot{p} = 0\ \forall k > 0$; (ii) if $p \in [0, \zeta)$, then

$$\lim_{k \to +\infty} \dot{p} \to +\infty;$$

(iii) if $p \in (\zeta, 1)$, then

$$\lim_{k \to +\infty} \dot{p} \to -\infty.$$

Equivalently, in the spirit of the Thikhonov's theorem [58,59], let us set in the fast timescale of eq. (2). This implies that one considers *frozen* both I and $\gamma(t)$ so that it is straightforward to verify that $\zeta(I, \gamma(t))$ is the only globally asymptotically stable equilibrium of (2) *at its timescale*. Thus, model (1)– (2) reduces to the following bidimensional model:

$$\dot{S} = \mu(1 - \zeta(I, \gamma(t))) - \beta SI - \mu S, \tag{6a}$$

$$\dot{I} = \beta SI - (\nu + \mu)I, \tag{6b}$$

with ζ given in (5). Model (6), from the control theory viewpoint [14,43], is a nonlinear controlled model

$$\dot{x} = F(x, u(t))$$

where $x = (S, I)$, $u(t) = \gamma(t)$, and F nonlinearly depends on the enacted control:

$$F(x, u(t)) \neq a(x)u(t) + b(x),$$

for given $a(\cdot)$, $b(\cdot)$, i.e. $F(x, u(t))$ is not a linear-affine function of $u(t)$. Note that the original system proposed in [9,10,18,62] was, instead, linearly dependent on $u(t) = \gamma(t)$.

More precisely, we may say that in this section we will deal with open-loop control of (6). Later on we will focus on one of the most important, especially for the health economy viewpoint, form of feedback control, i.e. optimal control [36,50].

In the important case of constant control $\gamma(t) = \gamma = const.$, model (6) belongs to the class of models proposed and investigated by d'Onofrio et al. [19], where the equation for S reads as follows

$$\dot{S} = \mu(1 - p_0 - p_1(I)) - \beta SI - \mu S,$$

and the baseline vaccination rate p_0, which is independent on the information received concerning the disease and the side effects of the vaccine, has a fundamental role. Indeed, in [19] it was shown that, by denoting with $\mathcal{R}_0 = \beta/(\nu + \mu)$ the SIR basic reproduction number, if

$$p_0 > p_c = 1 - \frac{1}{\mathcal{R}_0}, \tag{7}$$

then the disease elimination is possible; if $p_0 < p_c$, instead, the disease-free equilibrium is unstable and an endemic equilibrium onsets. Note that p_c is the May Anderson elimination threshold in presence of mandatory vaccination. It is clear that, in absence of a PHS intervention, a typical target population is unlikely to be characterized by a p_0 larger than the elimination threshold in presence of mandatory vaccine. Here, the baseline behaviour-independent vaccination rate p_0 introduced in [19] is better explained. Indeed, it is equal to

$$p_0 = \zeta(0, \gamma),$$

i.e. $p_0 = p_0(\gamma)$ is an increasing function of γ. Thus, proceeding similarly to [19] (where p_0 was constant), an appropriately intense awareness campaign might induce the disease elimination provided that

$$p_0(\gamma) > 1 - \frac{1}{\mathcal{R}_0},$$

i.e.

$$\gamma > p_0^{-1}(p_c). \tag{8}$$

From the control theory viewpoint, we may say that if (8) holds, then the open-loop constant control globally stabilizes the disease-free equilibrium (DFE).

In the case where the open-loop control $\gamma(t)$ is not constant, but $\gamma_{\min} \leq \gamma(t) \leq \gamma_{\max}$, with $\gamma_{\min} < \gamma_{\max} < +\infty$, we get straightforwardly that: (i) if

$$p_0(\gamma_{\min}) > 1 - \frac{1}{\mathcal{R}_0},$$

then the DFE is globally attractive; (ii) if

$$p_0(\gamma_{\max}) < 1 - \frac{1}{\mathcal{R}_0},$$

then the DFE is unstable.

An interesting special case is when $\gamma(t)$ is periodic, which mimics the alternance of the work and holidays terms in the PH interventions. Namely, it is easy to show (see Appendix A) that, denoting as $Y_\infty(t)$ the periodic solution of

$$\dot{Y} = \mu(1 - \zeta(0, \gamma(t)) - Y),$$

it holds that if

$$\mathcal{R}_0 \frac{1}{T} \int_0^T Y_\infty(t)dt < 1,$$

i.e. if

$$\mathcal{R}_0 \left(1 - \frac{1}{T} \int_0^T \zeta(0, \gamma(t))dt\right) < 1, \tag{9}$$

then the disease-free solution is globally attractive, whereas if

$$\mathcal{R}_0 \left(1 - \frac{1}{T} \int_0^T \zeta(0, \gamma(t))dt\right) > 1,$$

then it is unstable.

Let us consider the case where $\gamma(t)$ assumes periodically only two values in $[0, T]$:

$$\gamma(t) = \begin{cases} \gamma_1 & \text{if } 0 \leq t \leq T_1 \\ \gamma_2 & \text{if } T_1 < t \leq T \end{cases}$$

This scenario mimics in the most schematic case a lower pressure of PHS during, for example, a single period of holidays. In such a case the elimination condition becomes

$$\zeta(0, \gamma_1)\frac{T_1}{T} + \zeta(0, \gamma_2)\left(1 - \frac{T_1}{T}\right) > 1 - \frac{1}{\mathcal{R}_0}. \tag{10}$$

It is easy to show that constraint (10) holds also in case of a more complex pattern of alternance between the two values γ_1 and γ_2, for example due to multiple holidays terms.

4. Applying optimal control theory to foster vaccine uptake

In the previous sections, we illustrated as the proposed ordinary differential equations (ODEs) model can be seen, in its general case, as an 'open-loop' controlled system. As it is well known, whenever possible, it is preferable to control a system by means of feedback-based strategy [14,43].

In health economy, probably the most important form of feedback-based control is optimal control, which is aimed at minimizing the economic and human burden of some health-related phenomena [24]. As a consequence, in this section we start investigating which are the implications of the current age of fast opinion switching on the determination of the optimal time profile for the awareness campaigns, summarized in the control variable $\gamma(t)$, so that the overall costs are minimized.

These costs include the following three components [11,12]: the costs due to the disease

$$J_d = K_d \int_0^T N\beta SIdt;$$

the costs due to the vaccination and its (although rare) side effects

$$J_v = K_v \int_0^T N\mu\zeta(I, \gamma(t))dt;$$

and the costs of enacting PH campaigns, J_γ.

As far as the last cost is concerned, we follow the approach of [12], where

$$J_\gamma = \int_0^T C_\gamma \rho(\gamma(t), A)\gamma(t) A dt \tag{11}$$

with $A = 1 - p$ and ρ verifying: $\partial_\gamma \rho > 0$, $\partial_A \rho < 0$, $\lim_{A\to 0^+} \rho = +\infty$ (for detailed motivations see [12]). Here, we rewrite (11) as follows:

$$J_\gamma = \int_0^T \frac{C_\gamma}{k} \rho(\gamma(t), A) k\gamma(t) A dt,$$

by considering that: (i) the flux of subjects switching from the strategy 'no vaccine' to the strategy 'vaccine' is $k\gamma(t)A$, (ii) since the opinion switching rate is very fast, the critical assumption is that the cost to make a person switches from 'NO' to 'YES' is accordingly low and of order $1/k$. The inverse proportionality w.r.t. k implies that the population-wide global cost is neither null nor infinite. Then, as in [12], we assume $\rho = \gamma(t)/A$, leading to

$$J_\gamma = \int_0^T C_\gamma \gamma^2(t) dt.$$

It is of interest to stress that the quadratic dependence of this cost component w.r.t. the control $\gamma(t)$ is not decided *a priori*, i.e. based on mathematical convenience, but based on reasoning on the phenomenon in study.

In sum, we are looking for the optimal control function $\gamma^*(t)$ that minimizes the objective functional

$$J(\gamma(t)) = \int_0^T \Big(C_d SI + C_v \zeta(I, \gamma(t)) + C_\gamma \gamma^2(t)\Big) dt, \tag{12}$$

where $C_d = K_d \beta N$, $C_v = K_v \mu N$, on the admissible set for the control $\gamma(t)$

$$\Omega = \Big\{\gamma(t) \in L^1(0, T) \,|\, \gamma_{\min} \le \gamma(t) \le \gamma_{max}\Big\}.$$

5. Candidate optimal control

According to Pontryagin minimum principle, if an optimal solution exists, then the optimal control $\gamma^*(t)$ minimizes the so-called *Hamiltonian* function pointwise w.r.t. the control [50]. Here, the Hamiltonian H reads:

$$H = C_d SI + C_v \zeta(I, \gamma(t)) + C_\gamma \gamma^2(t) + \lambda_1[\mu(1 - \zeta(I, \gamma(t))) - \mu S - \beta SI] + \lambda_2[\beta SI - (\mu + \nu)I] \tag{13}$$

where $\lambda = (\lambda_1, \lambda_2)$ is the solution vector of the *adjoint system*

$$\dot\lambda_1 = -C_d I + (\lambda_1 - \lambda_2)\beta I + \mu\lambda_1,$$
$$\dot\lambda_2 = \begin{cases} -C_d S + (\lambda_1 - \lambda_2)\beta S + \lambda_2(\mu + \nu) + W & \text{if } f(I, \gamma(t)) < 1 \\ -C_d S + (\lambda_1 - \lambda_2)\beta S + \lambda_2(\mu + \nu) & \text{if } f(I, \gamma(t)) \ge 1 \end{cases}$$

with

$$W = \frac{\lambda_1\mu - C_v}{2\alpha} \partial_I \theta(I) \left(1 + \frac{\theta(I)}{\sqrt{\theta^2(I) + 4\alpha\gamma(t)}}\right),$$

and *transversality conditions*

$$\lambda(T) = 0. \tag{14}$$

The existence of the solution for our OC problem is not provided by classical existence theorems [21,36,39,53], whose requirements are not satisfied here. In particular, it is not guaranteed that the velocity sets

$$F_\gamma(S, I) = \{F(S, I, \gamma(t)) \,|\, \gamma(t) \in [\gamma_{\min}, \gamma_{\max}]\},$$

where F is the r.h.s. of (6), are convex for every (S, I). Hence, there is no analytical evidence (to the best of our knowledge) that the derivation of the constrained minimum point of H at each time instant t can provide us the 'true' minimizing control. Nonetheless, the $\gamma(t)$ obtained by applying the interpolation procedure can be considered at least a useful starting point for numerical computations. In other words, we can call it a *candidate* optimal control.

In order to derive the minimum point of H at each time instant t, we must distinguish the following three cases:

- If $\theta(I) \ge \alpha$, then $f(I, \gamma(t)) \ge 1$ and H is increasing w.r.t. $\gamma(t)$. Hence,
$$\gamma^*(t) = \gamma_{\min}. \tag{15}$$
- If $\theta(I) < \alpha$ and $C_v - \lambda_1\mu \ge 0$, then
$$\partial_\gamma H = \begin{cases} 2C_\gamma\gamma(t) + (C_v - \lambda_1\mu)\frac{1}{\sqrt{\theta^2(I) + 4\alpha\gamma(t)}} & \text{if } \gamma(t) < \alpha - \theta(I) \\ 2C_\gamma\gamma(t) & \text{if } \gamma(t) \ge \alpha - \theta(I) \end{cases} \tag{16}$$
namely, H is increasing w.r.t. $\gamma(t)$ and also for such instants the (15) holds.

- If $\theta(I) < \alpha$ and $C_v - \lambda_1\mu < 0$, then from (16) it follows that H is an increasing function of $\gamma(t)$ in the time interval when $\gamma(t) \geq \alpha - \theta(I)$. Otherwise, if $\gamma(t) < \alpha - \theta(I)$, H can still be increasing or have a minimum point, that is the unique solution of:

$$2C_\gamma \gamma(t)\sqrt{\theta^2(I) + 4\alpha\gamma(t)} = \lambda_1\mu - C_v \tag{17}$$

namely, the intersection point of an increasing function of $\gamma(t)$ (the l.h.s. of (17)) and a constant function (the r.h.s of (17)). Note that the (17) is equivalent to the cubic equation:

$$4\alpha\gamma^3(t) + \theta^2(I)\gamma^2(t) - \left(\frac{\lambda_1\mu - C_v}{2C_\gamma}\right)^2 = 0, \tag{18}$$

that can be explicitly solved (see Appendix B). Denote with $\tilde{\gamma}(t)$ the solution of (17), then

$$\gamma^*(t) = \begin{cases} \min\left(\max\left(\gamma_{\min}, \tilde{\gamma}(t)\right), \gamma_{\max}\right) & \text{if } \tilde{\gamma}(t) < \alpha - \theta(I) \\ \min\left(\max\left(\gamma_{\min}, \alpha - \theta(I)\right), \gamma_{\max}\right) & \text{if } \tilde{\gamma}(t) \geq \alpha - \theta(I) \end{cases}$$

Summarizing, we may say that the above procedure provides us with the following candidate optimal control:

$$\gamma^*(t) = \begin{cases} \gamma_{\min} & \text{if } \theta(I) \geq \alpha \text{ or } (\theta(I) < \alpha \text{ and } C_v - \lambda_1\mu \geq 0) \\ \min\left(\max\left(\gamma_{\min}, \tilde{\gamma}(t)\right), \gamma_{\max}\right) & \text{if } \theta(I) < \alpha \text{ and } C_v - \lambda_1\mu < 0 \text{ and } \tilde{\gamma}(t) < \alpha - \theta(I) \\ \min\left(\max\left(\gamma_{\min}, \alpha - \theta(I)\right), \gamma_{\max}\right) & \text{if } \theta(I) < \alpha \text{ and } C_v - \lambda_1\mu < 0 \text{ and } \tilde{\gamma}(t) \geq \alpha - \theta(I) \end{cases}$$

Observe that conditions (14) imply that $C_v - \lambda_1(T)\mu = C_v \geq 0$, yielding

$$\gamma^*(T) = \gamma_{\min}. \tag{19}$$

For convenience of notation, in the following we will omit the use of superscript * for the optimal control function.

6. Parametrization and simulations scenarios

In order to make comparisons with the 'slower' imitation speed model, studied by Buonomo et al. [12], we choose the same parameter values, that are listed and described in Table 1, and assume

$$\theta(I) = \theta_0 + \theta_1 I,$$

with θ_0 and θ_1 non-negative constants. In particular, we consider five possible simulation scenarios that differ for the combination of the rate of perceived risk of infection θ_1 and the maximum intervention level $\gamma_{\max}$ and should capture all the relevant situations:

- **C1** $(\theta_1, \gamma_{\max}) = (2000 \text{ days}^{-1}, 0.7\alpha p_c^2)$, corresponding to a large perceived relative risk of infection and a high level of intervention;
- **C2** $(\theta_1, \gamma_{\max}) = (450 \text{ days}^{-1}, 0.5\alpha p_c^2)$, corresponding to intermediate perceived relative risk of infection and level of intervention;
- **C3** $(\theta_1, \gamma_{\max}) = (450 \text{ days}^{-1}, 0.7\alpha p_c^2)$, corresponding to an intermediate perceived relative risk of infection and a high level of intervention;
- **C4** $(\theta_1, \gamma_{\max}) = (4000 \text{ days}^{-1}, 0.5\alpha p_c^2)$, corresponding to a very large perceived relative risk of infection and an intermediate level of intervention;
- **C5** $(\theta_1, \gamma_{\max}) = (4000 \text{ days}^{-1}, 0.7\alpha p_c^2)$, corresponding to a very large perceived relative risk of infection and a high level of intervention.

Remind that in the 'slower' imitation speed model with $\gamma(t) = \gamma = const.$ the threshold $\gamma = \alpha p_c^2$ would ensure elimination [12].

As in [4,11,12], we also include a small immigration/emigration constant flux ε to take into account the immigration of infected individuals during inter-epidemic periods. Precisely, a positive influx $+\varepsilon$ is added to the eq. (6b), balanced by a negative term $-\varepsilon$ in the eq. (6a). Clearly, this constant influx term must be taken into account also in (13).

As far as the optimal control is concerned, the most specific parameter is C_γ, because it defines the weight of the communication strategy cost w.r.t. the other costs. We will use two values: a baseline value $C_\gamma = C_\gamma^{(o)}$ and a larger value $C_\gamma = 5C_\gamma^{(o)}$. The latter is employed to assess how the control changes in the case of substantially larger costs for the Public Health campaigns aimed at increasing the propensity to vaccinate.

7. Numerical optimal solution by FBS and gradient descent algorithms

In mathematical epidemiology, two widely adopted algorithms for the numerical OC solutions are the forward-backward sweep (FBS) method [39] and the gradient descent or steepest descent (Grad) method [2] (which can also be employed for the OC of spatio-temporal models [32]). Their interest lies on the fact that: (i) both of them are based on the Pontryagin

Table 1
Epidemiological, behavioural and control-related parameters values.

Parameter	Description	Baseline value
μ	Natural birth/death rate	1/50 years^{-1}
ν	Recovery rate	1/10 days^{-1}
$\mathcal{R}_0$	Basic reproduction number	10
β	Transmission rate	$\mathcal{R}_0(\mu+\nu)$
p_c	Critical immunization threshold	$1-1/\mathcal{R}_0$
ε	Emigration/immigration flux	2.86×10^{-8} days^{-1}
α	Rate of perceived risk of vaccine side effects	1 days^{-1}
θ_0	Minimum perceived risk of infection	0 days^{-1}
θ_1	Rate of perceived risk of infection	450–4000 days^{-1}
N	Total population	6×10^7
T	Length of the planning horizon	10 years
$\gamma_{\min}$	Minimum rate of efforts into awareness campaigns	0 days^{-1}
$\gamma_{\max}$	Maximum rate of efforts into awareness campaigns	$0.5\alpha p_c^2-0.7\alpha p_c^2$
K_d	Average unit cost per infectious case	307 USD
K_ν	Average unit cost of vaccination	21.08 USD
C_d	Total cost of infection	$K_d\beta N$
C_ν	Total cost for vaccination	$K_\nu\mu N$
$C_\gamma^{(o)}$	Cost for implementation of awareness campaigns	$N\mu K_\nu/(\alpha^2 p_c^3)$

Table 2
Case $C_\gamma = C_\gamma^{(o)}$: quantities measuring the differences between the OC solutions by deterministic methods (FBS and Grad) and by one iteration of heuristic algorithms (PSO and DE). Outputs by FBS method are used as reference. Parameter values and initial data as in Fig. 3.

Scenario	Method	$\frac{\\|\gamma(t)-\gamma_{FBS}(t)\\|_1}{\\|\gamma_{FBS}(t)\\|_1}$	J (USD)	$\frac{J-J_{FBS}}{J_{FBS}}$	J_γ (USD)	$\frac{J_\gamma-J_{\gamma\cdot FBS}}{J_{\gamma\cdot FBS}}$
C1	FBS	0	6.51×10^8	0	1.03×10^8	0
	Grad	4.28×10^{-3}	6.51×10^8	2.27×10^{-4}	1.03×10^8	-1.71×10^{-3}
	PSO	7.36×10^{-3}	6.51×10^8	6.16×10^{-4}	1.04×10^8	3.28×10^{-3}
	DE	3.17×10^{-2}	6.55×10^8	6.19×10^{-3}	1.06×10^8	2.06×10^{-2}
C2	FBS	0	1.12×10^9	0	5.53×10^7	0
	Grad	1.75×10^{-7}	1.12×10^9	-2.59×10^{-7}	5.53×10^7	3.07×10^{-7}
	PSO	3.51×10^{-3}	1.12×10^9	1.04×10^{-4}	5.55×10^7	3.11×10^{-3}
	DE	3.51×10^{-3}	1.12×10^9	1.04×10^{-4}	5.55×10^7	3.11×10^{-3}
C3	FBS	0	7.84×10^8	0	1.04×10^8	0
	Grad	1.49×10^{-4}	7.84×10^8	2.24×10^{-7}	1.04×10^8	-1.19×10^{-4}
	PSO	6.37×10^{-3}	7.85×10^8	3.15×10^{-4}	1.04×10^8	2.31×10^{-3}
	DE	6.37×10^{-3}	7.85×10^8	3.15×10^{-4}	1.04×10^8	2.34×10^{-3}
C4	FBS	0	7.00×10^8	0	5.43×10^7	0
	Grad	3.69×10^{-4}	7.00×10^8	8.76×10^{-6}	5.44×10^7	4.11×10^{-4}
	PSO	7.97×10^{-3}	7.00×10^8	4.76×10^{-4}	5.43×10^7	-6.44×10^{-4}
	DE	3.76×10^{-2}	7.16×10^8	2.31×10^{-2}	5.25×10^7	-3.40×10^{-2}
C5	FBS	0	5.67×10^8	0	1.01×10^8	0
	Grad	1.60×10^{-3}	5.67×10^8	7.47×10^{-5}	1.01×10^8	-4.20×10^{-4}
	PSO	9.04×10^{-3}	5.67×10^8	1.16×10^{-3}	1.01×10^8	3.71×10^{-3}
	DE	2.09×10^{-2}	5.69×10^8	3.33×10^{-3}	1.04×10^8	2.89×10^{-2}

Hamiltonian, and – as such – they aim to numerically solve the Pontryagin's differential-algebraic boundary value problems [50]; (ii) they are recursive algorithms, thus they are easy to be implemented and do not require the use of special type libraries, at variance with numerical methods to solve boundary value problems such as the multiple shooting method [48]. Note that the point (i) implies that both the FBS and the Grad methods fully take advantage of the analytical results of OC theory, which is very appreciable.

As mentioned above, for our control problem one has no guarantee that Pontryagin necessary conditions of optimality are also sufficient. However, the above algorithms can be used as well. Namely, we numerically investigate our OC problem 'as if' the optimality sufficient conditions would hold. Specifically, we employ the public domain routines for the FBS and for the Grad method provided, respectively, by Lenhart and Workman [39] and by Aniţa et al. [2] for the Matlab environment [44]. As far as the numerical resolution of the differential equations in concerned, we employ the fourth-order Runge–Kutta method with constant step size, as in [39].

We observe that for $C_\gamma = C_\gamma^{(o)} = N\mu K_\nu/(\alpha^2 p_c^3)$ both the above-mentioned algorithms converge to numerical solutions whose difference is very small. This suggests that – in the numerical cases we are analyzing – the 'candidate' optimal control is in reality the optimal control. On the contrary, for $C_\gamma = 5C_\gamma^{(o)}$ both algorithms are not able to converge in all the scenarios we consider.

The case $C_\gamma = C_\gamma^{(o)}$ is numerically summarized in Table 2, where FBS method is used as reference and the corresponding quantities are labelled with subscript $_{FBS}$. Moreover, panels in Fig. 1 show the OC solutions, obtained by means of the FBS

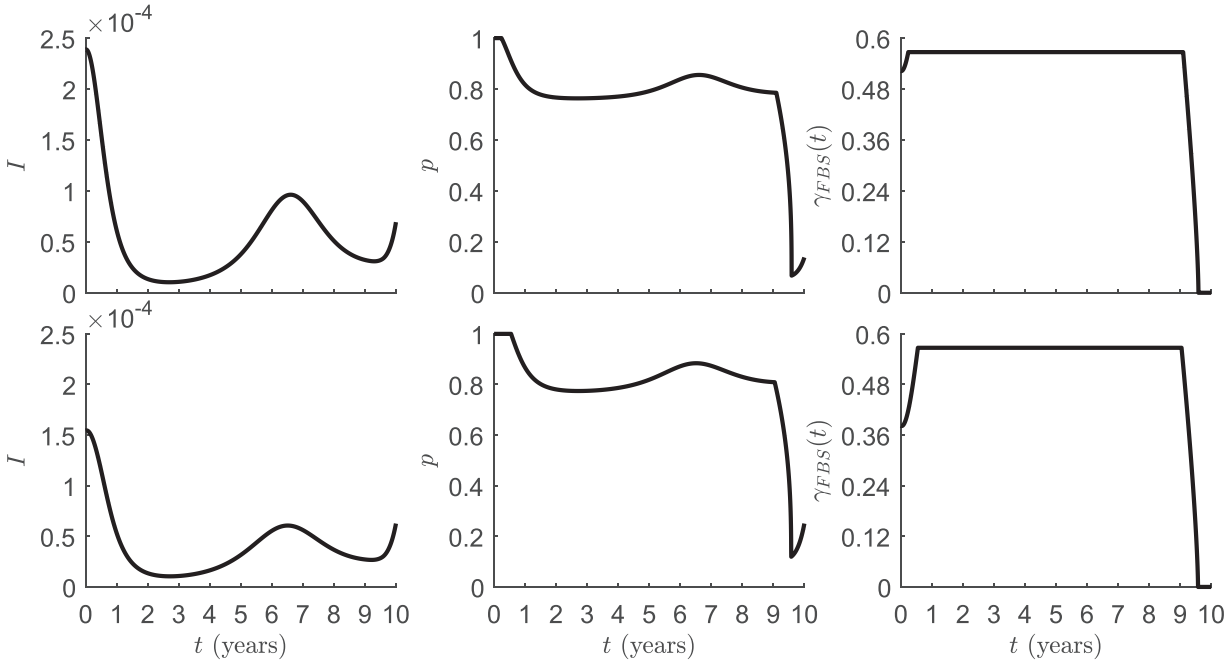

Fig. 1. OC solutions by FBS method for the simulation scenarios C1 (top row) and C5 (bottom row). Left panels: I; central panels: p; right panels: $\gamma_{FBS}(t)$. Initial data as in [12], that is: $S(0) = 0.0999972$, $I(0) = 2.3878 \times 10^{-4}$ for the case C1; the endemic equilibrium of model (6) with $\gamma(t) \equiv 0$ for the case C5. Other parameter values are listed in Table 1.

algorithm [39], for different combinations of θ_1 and $\gamma_{\max}$, which correspond to the cases C1 (top panels) and C5 (bottom panels) (for the other cases see Fig. S1 in Supplementary Materials). The results are quite similar to those of [12], but here the optimal control has an initial increasing behaviour, especially in case C5. Anyway, we obtain that $\gamma(t) \approx \gamma_{\max}$ for most of the horizon, suggesting that the cost for the implementation of awareness campaigns, $C_\gamma^{(0)}$, is relatively low, so that it is preferable to maintain a maximum control rate as far as it is possible (reminding the terminal condition (19)). The importance of remaining for most time at the largest possible effort to minimize the costs is, however, non trivial from the Public Health viewpoint, because one could be tempted to relax the efforts in periods of large vaccine uptake and/or low prevalence of the disease. The message of our simulations is that this would not be a good index since sooner or later an excessive increase of the prevalence would increase the costs. Moreover, decrease of the vaccine uptake would surely occur.

7.1. Robustness of the FBS optimal control to periodic perturbations

As it is well-known, the Pontryagin principle does not ensure that the control function obtained by applying it is an actual global minimum. Thus, in order to validate the global optimality of the candidate solution yielded by the Pontryagin necessary conditions, we first consider a very simple heuristic approach. The approach consists in assessing the robustness of the candidate optimal control $\gamma_{FBS}(t)$ (numerically obtained by the FBS method) to sinusoidal perturbations of various amplitudes and periods:

$$\gamma_{pert}(t) = \min\left(\max\left(\gamma_{\min}, \gamma_{FBS}(t)\left(1 + A\sin\left(\frac{2\pi}{\tau}t\right)\right)\right), \gamma_{\max}\right),$$

with $A \in [-1/2, 1/2]$ and $\tau \in [0, 10]$ years. Numerical results are displayed in Fig. 2 for the case C4 and in Fig. S2 of Supplementary Materials for the other cases. We report the values of

$$J_{pert} = J(\gamma_{pert}(\cdot))$$

normalized w.r.t. $J_{FBS} = J(\gamma_{FBS}(\cdot))$, as function of the amplitude A and the period τ. As one can notice, in all cases it is

$$J(\gamma_{pert}(\cdot)) > J(\gamma_{FBS}(t)),$$

suggesting that the algorithm might have found a global optimum.

8. Numerical optimal solution by heuristic global optimization algorithms

As we mentioned in the previous section, in the cases where $C_\gamma = 5C_\gamma^{(o)}$, both FBS and Grad algorithms incur in problems of convergence. The FBS and the gradient descent method belong, similarly to the single and multiple shooting methods [48],

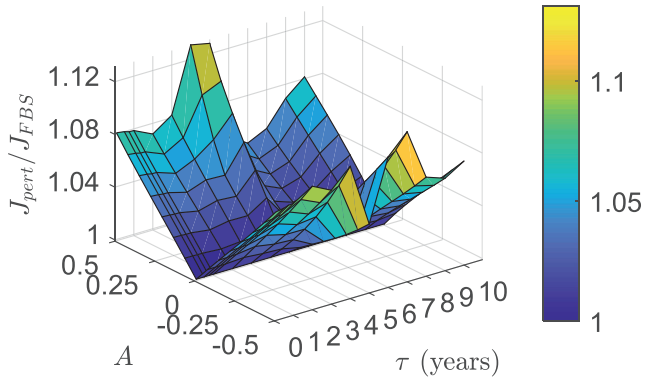

Fig. 2. J_{pert}/J_{FBS} as function of A and τ for the simulation scenario C4. Initial data: endemic equilibrium of model (6) for $\gamma(t) \equiv 0$. Other parameter values are listed in Table 1.

to the class of indirect optimization methods. In other words, they are based on the Pontryagin Hamiltonian, i.e. they take advantage of the available variational solution of the OC problem expressed as a boundary value problem for a differential-algebraic (DA) system.

In OC theory and applications, also many deterministic algorithms based on the direct optimization of the objective functional are available [20,28,61]. Note that often a relationship between direct methods and the solution of the Pontryagin DA system can be shown, as in [23]. Nonetheless, similarly to FBS and the Grad algorithms, the deterministic direct optimization approach does not ensure that the found solution actually corresponds to a genuine global minimum.

Thus, in order to solve our OC problem in the cases where $C_\gamma = 5C_\gamma^{(o)}$, we recur to direct optimization by applying two stochastic heuristic global optimization algorithms (HOAs). These algorithms are conceived to directly solve general optimization problems and, as such, they are not related to OC theory.

A major difference between the heuristic optimization algorithms and the OC-specific algorithms is that the first ones are aimed to finite dimensional problems, the second ones to infinite dimensional problems. However, the latter any case operate a discretization, i.e. the reduction to a finite dimensional space, although of 'large' dimension due to the small time step usually adopted. Another difference w.r.t. the FBS and the Grad methods as well as other direct optimization algorithms used in OC is that the heuristic optimization algorithms we have chosen are stochastic. It is the stochasticity that allows to significantly increase the probability that the minimum they find is a global minimum and not a local one. We will return later on some important implications of the stochasticity of these algorithms. Thus, even for $C_\gamma = C_\gamma^{(o)}$, we apply the HOAs to further validate the results obtained by the FBS and Grad methods.

When using heuristic approaches one has to transform the initial infinite dimensional approach in a finite dimensional problem. This, however, is not a heavy constraint for the OC problem to be solved. Indeed: (i) even the OC-specific algorithms operate a discretization, i.e. also they are finite dimensional; (ii) in the light of the lack of flexibility in PH interventions, this assumption provides OC solutions that are more realistic. In other words, 'real world' campaigns cannot be updated continuously in time, thus a piecewise-constant $\gamma(t)$ is more realistic than a continuous control. Namely, we assume that the communication campaigns enacted by the PHS are updated every three months, i.e. at each new season. This implies 40 discretization points for the whole control horizon $[0, 10]$ years, and, of course, that the $\gamma(t)$ is a piecewise-constant function.

As far as the global optimization algorithms are concerned, we employ the following two widely diffused algorithms:

- Particle swarm optimization (PSO). This algorithm was originally described by Kennedy and Eberhart [35]. Recent versions include subsequent modifications suggested in [46,49]; a generalization involving the adoption of complex-order derivatives is given by Machado et al. [41]. We use the `particleswarm` solver included in the *Global Optimization Toolbox* of Matlab [44]. We employ the default option values, except for the termination tolerance on the function value (`FunctionTolerance`) and the maximum number of iterations allowed (`MaxIterations`), that we set to 10^{-5} and 200, respectively. The PSO algorithm is based on the concept of swarm intelligence, i.e. the emergent 'pseudo-intelligent' behaviour emerging at the collective level in swarms of individuals that follow simple laws of interactions between them and the surrounding environment [35,46,49].
- Differential evolution (DE). It was first proposed by Storn [56] and subsequently improved by Storn and Price [57]. We use the algorithm described by Price et al. [52] and implement the Matlab code provided in [51]. We employ the default algorithm options, except for the number of population members (I_NP) and the maximum number of generations until optimization stops (I_itermax), that are set to 50 and 800, respectively.

For a description of the above algorithms and further details, please refer to [7]. Our aim here is not to compare their performances. This would be out of our competences and, moreover, a conspicuous number of papers have already investigated this point, for example [13,15,60] (and references therein). The choice of PSO and DE algorithms is motivated by

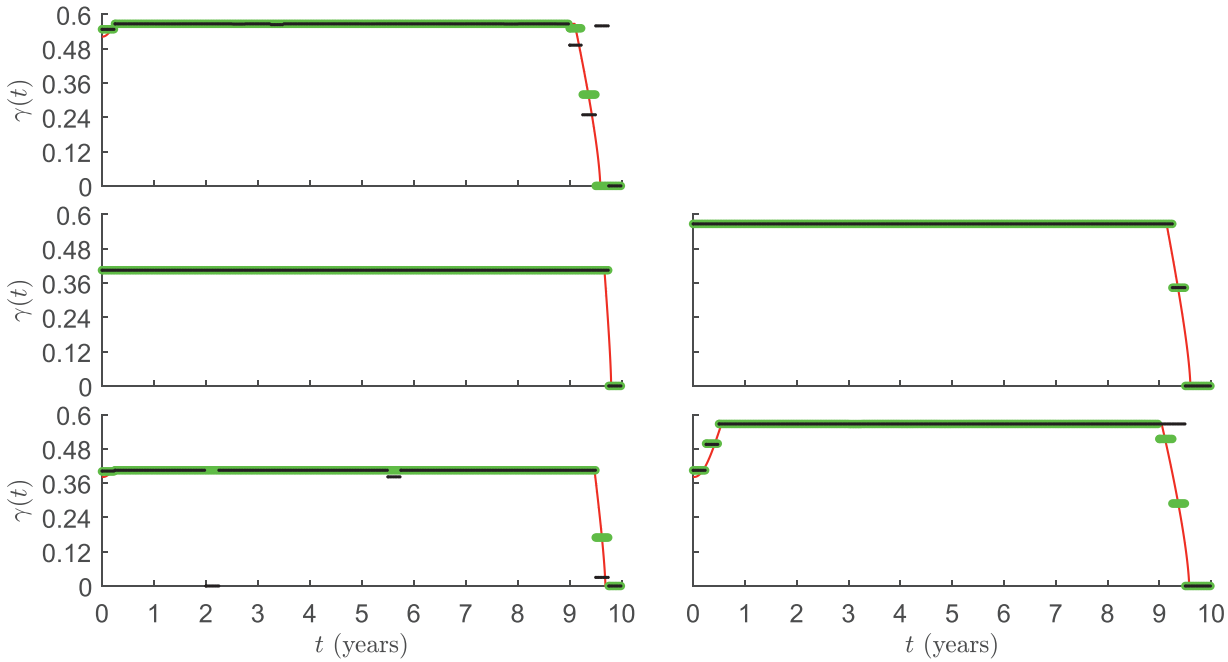

Fig. 3. Case $C_\gamma = C_\gamma^{(o)}$: OC function $\gamma(t)$ by FBS method (red lines) and one iteration of PSO (green lines) and DE (black lines) algorithms. Left panels, from the top to bottom: cases C1, C3 and C5, respectively. Right panels, from the top to bottom: cases C2 and C4, respectively. Initial data as in [12], that is: $S(0) = 0.0999972$, $I(0) = 2.3878 \times 10^{-4}$ for the case C1; the endemic equilibrium of model (6) with $\gamma(t) \equiv 0$ for the other cases. Other parameter values are listed in Table 1. (For interpretation of the references to colour in this figure legend, the reader is referred to the web version of this article.)

their excellent reputation within the domain of machine intelligence and cybernetic. Moreover, both algorithms do not need any gradient information of the function to be optimized, are conceptually very simple and they require minimal parameter tuning [7,15].

As far as the case $C_\gamma = C_\gamma^{(o)}$ is concerned, for each combination of θ_1 and $\gamma_{\max}$ considered, we compare both qualitatively (Fig. 3) and quantitatively (Table 2) the outputs of the PSO and of the DE algorithms w.r.t. the output of the FBS method. Both DE and PSO algorithms provide optimal controls that are on the whole very close to the ones provided by the FBS method (in turn very close to the ones obtained by the Grad method). However, the output of DE algorithm has sometime large local deviations. This suggests that some degree of flexibility in the implementation of the control does not dramatically change the results. Graphics and data values suggest that, for the specific problem at hand, the PSO algorithm performs slightly better than the DE algorithm.

As far as the case $C_\gamma = 5C_\gamma^{(o)}$ is concerned, we obtain a radically different OC solutions compared with the simulations where $C_\gamma = C_\gamma^{(o)}$, as shown in Fig. 4 (left panels). Indeed, in all cases the obtained control is strongly non-monotone. Moreover, for both the cases $C_\gamma = C_\gamma^{(o)}$ and $C_\gamma = 5C_\gamma^{(o)}$, PSO algorithm converges in shorter times than DE. The non-monotone nature of the control has an important implication from the Public Health standpoint: the structure that implements the vaccine awareness campaigns must be ready to relatively frequent adjustments of effort if one wants to minimize the total costs.

Let us now compare Fig. 4 (left panels) with Table 3. On the one hand, in Table 3 the relative difference of the optimal total costs J obtained with the two algorithms is in all cases very small. On the other hand, in Fig. 4 the optimal control obtained by the DE algorithms seems affected by large 'noise' w.r.t. the optimal $\gamma(t)$ obtained by PSO algorithm. On the whole, these results suggest that the system is robust with respect to even large local deviations from the theoretical optimal solution. In other words, the irregular additional stochastic oscillations in the optimal control obtained by DE algorithm suggest that a large degree of deviation is possible when implementing the optimal control. This is a very positive result from the Public Health viewpoint, because the robustness guarantees that the system can well react to temporary problems in the implementation of the vaccine awareness campaigns.

8.1. Alternative long-term schedules of PHS awareness campaigns

As we said in the previous sections, actual awareness campaigns are not continuous, but they vary in a piecewise-constant fashion. We have seen that, assuming a three months-based update, we obtain, under PSO, a discretized $\gamma(t)$ that is sufficiently close to a continuous control. By adopting DE, we obtain a more noisy solution. Here, we want to ex-

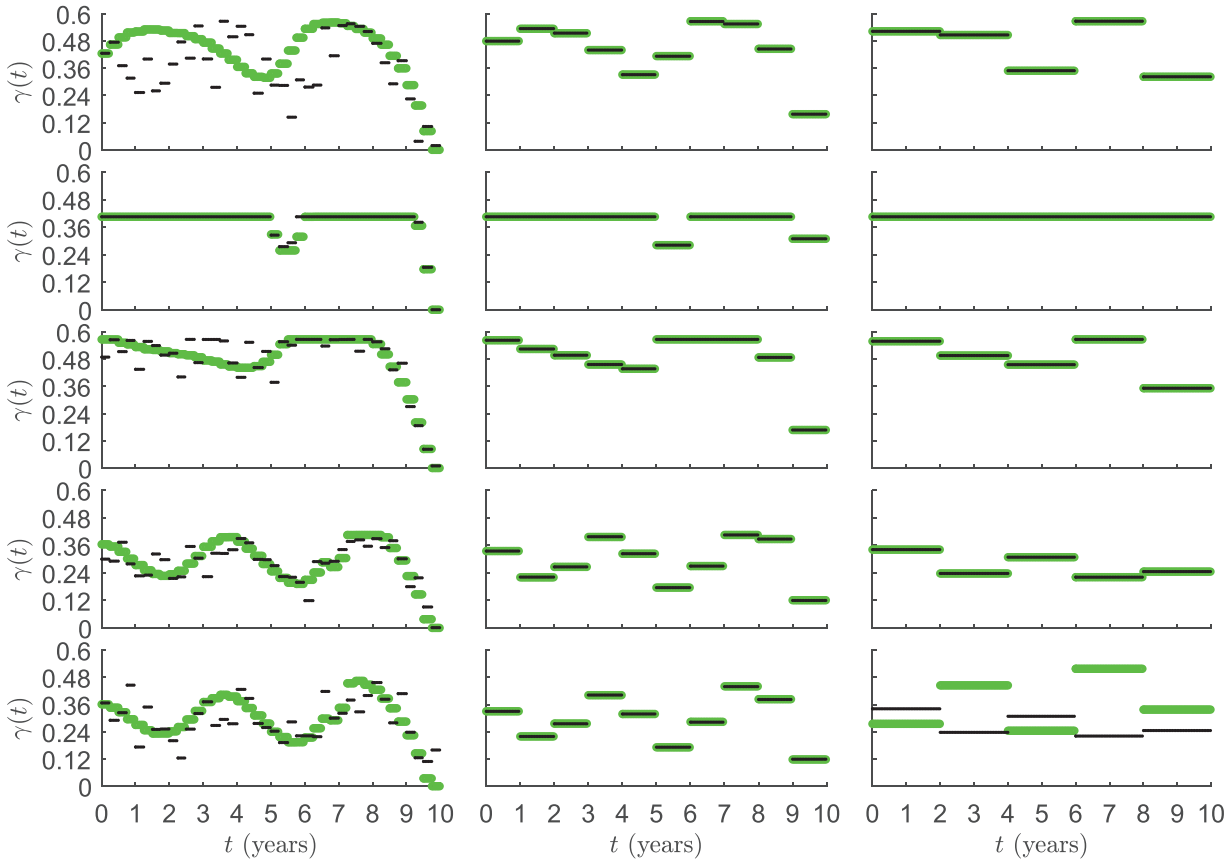

Fig. 4. Case $C_\gamma = 5C_\gamma^{(o)}$: optimization by one iteration of PSO (green lines) and DE (black lines) algorithms. OC function $\gamma(t)$ with 3 months (left panels), 1 year (central panels) and 2 years (right panels) programming. Rows, from the top to bottom: cases C1, C2, C3, C4 and C5, respectively. Parameter values and initial data as in Fig. 3. (For interpretation of the references to colour in this figure legend, the reader is referred to the web version of this article.)

Table 3
Case $C_\gamma = 5C_\gamma^{(o)}$: optimization by one iteration of PSO and DE algorithms. Costs J and J_γ for three different temporal control-updates (3 months, 1 year, 2 years). Parameter values and initial data as in Fig. 3.

Scenario	Method	3 months programming		1 year programming		2 years programming	
		J (USD)	J_γ (USD)	J (USD)	J_γ (USD)	J (USD)	J_γ (USD)
C1	PSO	1.01×10^9	3.56×10^8	1.02×10^9	3.65×10^8	1.03×10^9	3.73×10^8
	DE	1.07×10^9	2.68×10^8	1.02×10^9	3.65×10^8	1.03×10^9	3.74×10^8
C2	PSO	1.33×10^9	2.57×10^8	1.34×10^9	2.58×10^8	1.35×10^9	2.85×10^8
	DE	1.33×10^9	2.61×10^8	1.34×10^9	2.58×10^8	1.35×10^9	2.85×10^8
C3	PSO	1.17×10^9	4.25×10^8	1.17×10^9	4.28×10^8	1.19×10^9	4.20×10^8
	DE	1.18×10^9	4.29×10^8	1.17×10^9	4.28×10^8	1.19×10^9	4.20×10^8
C4	PSO	8.77×10^8	1.58×10^8	8.83×10^8	1.60×10^8	9.04×10^8	1.31×10^8
	DE	8.84×10^8	1.50×10^8	8.83×10^8	1.61×10^8	9.04×10^8	1.31×10^8
C5	PSO	8.76×10^8	1.67×10^8	8.83×10^8	1.67×10^8	9.05×10^8	2.48×10^8
	DE	8.90×10^8	1.60×10^8	8.83×10^8	1.66×10^8	9.04×10^8	1.31×10^8

plore the impact of even less flexible policies of intervention to favour vaccination. Namely, we will consider two additional scenarios:

- Yearly programming. We suppose that the PH interventions are updated once per year, for logistic and administrative reasons. For example the PH policies could depend on the budget law, which is changed on yearly basis;
- Biennial programming. This must not seem an extreme academic case. For example, in Soviet Union, during the leadership of Stalin, key policies actions were regulated by 'quinquennial plans'.

We only simulate the case $C_\gamma = 5C_\gamma^{(o)}$, where the three-months discretized optimal $\gamma(t)$ obtained by heuristic methods is oscillating. We obtain that, if the three-months optimal solutions are oscillating (i.e. scenarios C1, C3, C4 and C5), the same holds for the one-year and two-years scheduling. This is a useful indication for the PHS: the necessity of re-arranging

the effort remains even with annual and biennial programming, if one wants to minimize the costs. Of course, the degree of oscillation is smaller for the one-year w.r.t. the three-months scheduling, and smaller for the two-years w.r.t. the one-year scheduling. In the scenario C2, where the optimal control is not oscillating for the three-months scheduling, we get that the two-years scheduling optimal control is predicted to be constant.

As far as the use of PSO versus DE is concerned, we note that, in scenario C5 for the two-years scheduling, the optimal control obtained by the DE method corresponds to a cost that is much smaller than the one found by applying PSO. Moreover, the two controls in such a scenario are very dissimilar. This suggests that PSO does not converge to the actual global minimum, but to a local minimum. This is a rare event but not impossible and confirms that our choice to adopt two different algorithms is appropriate. In all other scenarios the outputs of PSO are very similar to the ones obtained by applying DE.

9. Statistical assessment of the OC solutions

Since heuristic and evolutionary algorithms are stochastic processes, they produce different outputs at each run. This has interesting implications. Indeed, each output is in principle an estimation of the true minimum, which comes from an unknown multivariate probability distribution. As a consequence, it is important to empirically infer statistical features of this distribution by repeated stochastic optimizations.

The problem is that, since the vectors to be estimated have a dimension that is quite large (40 in the case of three-months scheduling), a fully satisfactory statistical assessment would require very large samples. This would imply computation resources that, unfortunately, are out of our possibilities. Thus, we only propose preliminary statistical assessments made with a relatively small sample, which, however, are of some interest. Namely, for each set of parameters and initial conditions, we perform $K \gg 1$ stochastic optimizations to solve our OC problem ($K = 100$ in the case of three-months scheduling and $K = 200$ in the cases of annual and biennial scheduling). Due to its relatively shorter computational times, we employ the PSO algorithm.

Specifically, we perform the following descriptive statistical assessments:

- Time-wise assessment: basic statistical features of $\gamma(t)$. For each t we compute the median $\gamma(t)$ and the total range over the results obtained in the K optimizations. In other words, let $\Gamma = (\gamma_1(t), \dots, \gamma_K(t))^T$ be the matrix having as row-vectors the obtained optimal functions at time t, and let us define $\Gamma^{sort} = Sort(\Gamma)$ the sort of Γ by columns. Then $\gamma_{\min}(t) = \Gamma_1^{sort}$, $\gamma_{med}(t) = (\Gamma_{K/2}^{sort} + \Gamma_{K/2+1}^{sort})/2$ and $\gamma_{\max}(t) = \Gamma_K^{sort}$, where Γ_i^{sort} denotes the ith row of Γ^{sort}. Note that these three 'pseudo' control functions by construction cannot intersect in isolated points (they can coincide on intervals or in the whole temporal horizon). Of course, since, due to the discretization, $\gamma(t)$ is piecewise-constant, even $\gamma_{\min}(t)$, $\gamma_{med}(t)$ and $\gamma_{\max}(t)$ are piecewise-constant.
- Global assessment: basic statistical features of J. Namely, let $J_{\min}$, J_{med} and $J_{\max}$ be, respectively, the minimum, median and maximum value of J obtained in the K stochastic minimizations, we plot the corresponding three controls (actually, due to the discretization, vectors) $\gamma(t)$, which we denote as $\gamma^J_{\min}(t)$, $\gamma^J_{med}(t)$ and $\gamma^J_{\max}(t)$. Note that, at variance with the previous case, these three control functions can intersect.
- For the case $C_\gamma = C_\gamma^{(o)}$, where the comparison with the results obtained by FBS method is possible, we perform the following assessments: (i) we sort the optimal controls obtained by PSO algorithm by their relative L^1 distance from $\gamma_{FBS}(\cdot)$:

$$\epsilon_\gamma = \frac{||\gamma(t) - \gamma_{FBS}(t)||_1}{||\gamma_{FBS}(t)||_1},$$

  and we plot the $\gamma(t)$ with the minimal ($\gamma^{\epsilon_\gamma}_{\min}(t)$), median ($\gamma^{\epsilon_\gamma}_{med}(t)$) and maximal ($\gamma^{\epsilon_\gamma}_{\max}(t)$) value of ϵ_γ; (ii) we plot the related histogram of the ϵ_γ; (iii) we plot the histogram of the relative error of the costs:

$$\epsilon_J = \frac{J - J_{FBS}}{J_{FBS}}.$$

- For the case $C_\gamma = 5C_\gamma^{(o)}$, where no comparison is possible with FBS method due to its lack of convergence, we plot the histogram of the distribution of J over the K stochastic optimizations.

The above described statistical inferences have also another meaning, i.e. to assess how much robust is the numerically inferred optimal control. This is a fundamental information for the practical implementation of the results of the optimal control. Indeed, since in the reality one could appreciably deviate from the theoretical results, it follows that a global optimum that has a large range is far more implementable than another with identical mean and a very small range.

As far as the case $C_\gamma = C_\gamma^{(o)}$ is concerned, numerical results in the most interesting scenarios are displayed in Figs. 5 and 6 (for the others see Figs. S3–S5 in Supplementary Materials). As far as the case $C_\gamma = 5C_\gamma^{(o)}$ is concerned, numerical results in the most interesting scenarios are displayed in Figs. 7–9 (for the others see Figs. S6–S17 in Supplementary Materials). Overall, the variance of the distributions both of the errors and of the time courses is very small. In particular, all the found optimal controls are very close to each other in time. At some time points, there are exceptionally outliers. In sum, although the sample is limited because of the above-mentioned computational restrictions, the statistical assessment suggests that the PSO algorithm converges to the actual global minimum.

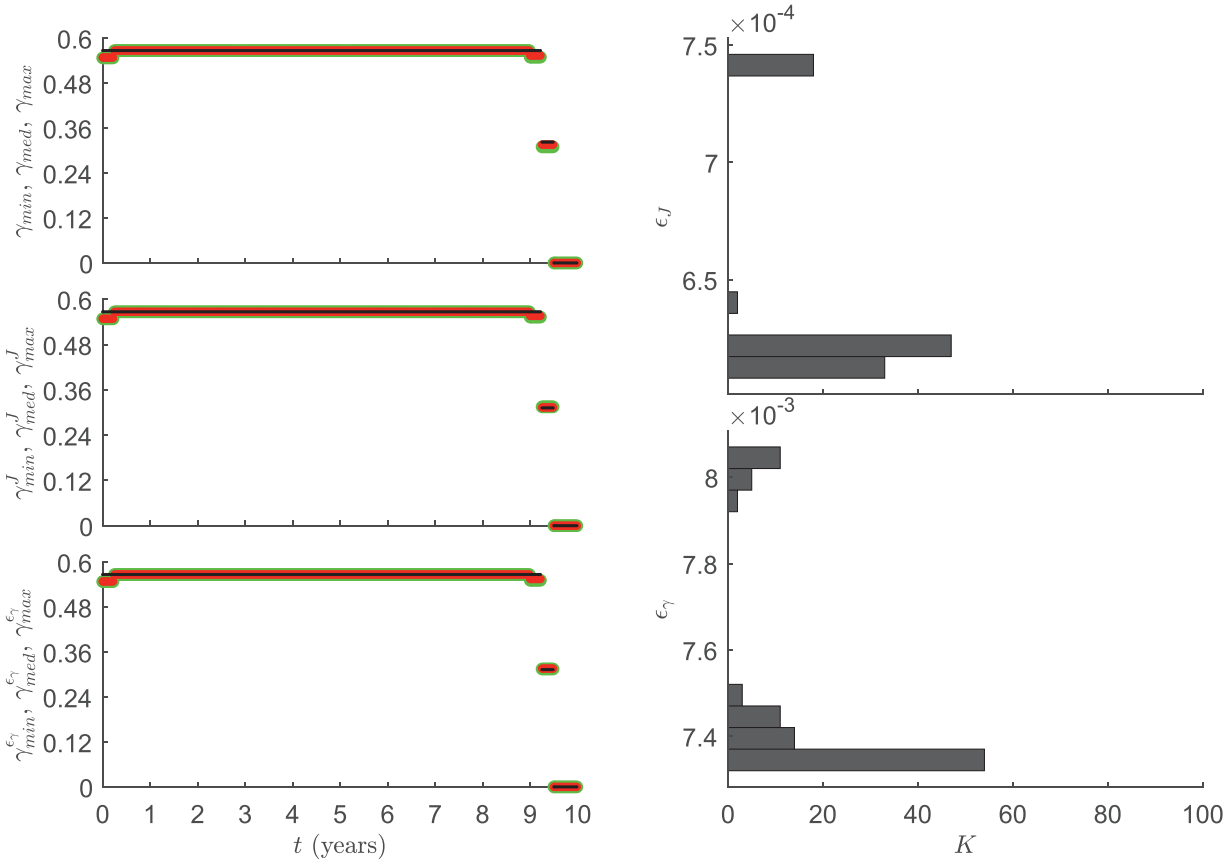

Fig. 5. Statistical assessment for the case $C_\gamma = C_\gamma^{(o)}$ and simulation scenario C1. Data obtained by applying $K = 100$ times the PSO algorithm. Left top panel: $\gamma_{\min}(t)$ (green line), $\gamma_{med}(t)$ (red line) and $\gamma_{\max}(t)$ (black line). Left central panel: $\gamma^J_{\min}(t)$ (green line), $\gamma^J_{med}(t)$ (red line) and $\gamma^J_{\max}(t)$ (black line). Left bottom panel: $\gamma^{\epsilon_\gamma}_{\min}(t)$ (green line), $\gamma^{\epsilon_\gamma}_{med}(t)$ (red line) and $\gamma^{\epsilon_\gamma}_{\max}(t)$ (black line). Right panels: distribution of ϵ_J (top panel) and of ϵ_γ (bottom panel). Parameter values and initial data as in Fig. 3. (For interpretation of the references to colour in this figure legend, the reader is referred to the web version of this article.)

10. Coming back to FBS method: non-convergence analysis

As we have seen, for $C_\gamma = 5C_\gamma^{(o)}$ the FBS and the Grad methods, both deterministic OC-oriented algorithms, have problems of convergence. Thus, we resort to two stochastic *general purpose* algorithms, PSO and DE. As a natural further step, we then employ the piecewise-constant OC solutions obtained by applying these two HOAs as an initial step for both the FBS and Grad methods. Namely, we set as hint values for the OC control to be determined the following ones

$$\gamma^{(0)}(t) = \gamma_{PSO}(t)$$

or

$$\gamma^{(0)}(t) = \gamma_{DE}(t),$$

where γ_{PSO} and γ_{DE} are the optimal solutions by one iteration of PSO and DE, respectively, as given in Fig. 4. The rationale in adopting these initial values for the control is that the HOAs find a piecewise-constant OC that ought to be, roughly speaking, quite close (in some suitable normed functional space) to the continuous optimum derived by the Pontryagin theory.

Again, we obtain that both setting $\gamma^{(0)}(t) = \gamma_{PSO}(t)$ and $\gamma^{(0)}(t) = \gamma_{DE}(t)$ the indirect optimization methods incur in convergence problems. To the best of our knowledge, the problem of the convergence of the FBS algorithm was first faced, theoretically and numerically, by McAsey et al. [45]. In that work, authors showed that FBS algorithm can fail to converge even facing the most 'simple' and analytically solvable OC problem: the minimization of a quadratic objective functional $J = \int_0^T (ax^2 + u^2(t))dt$ of the scalar linear controlled ODE $\dot{x} = bx + u(t)$. Namely, they reported that for $(a, b) = (3, 1)$ the algorithm does not converge and it enters in a periodic loop of period 2.

This makes the use of heuristic stochastic optimization methods (the ones we employ or others, such as the simulated annealing) very attractive in all cases where FBS or Grad or other deterministic algorithms fail to converge. Moreover, even

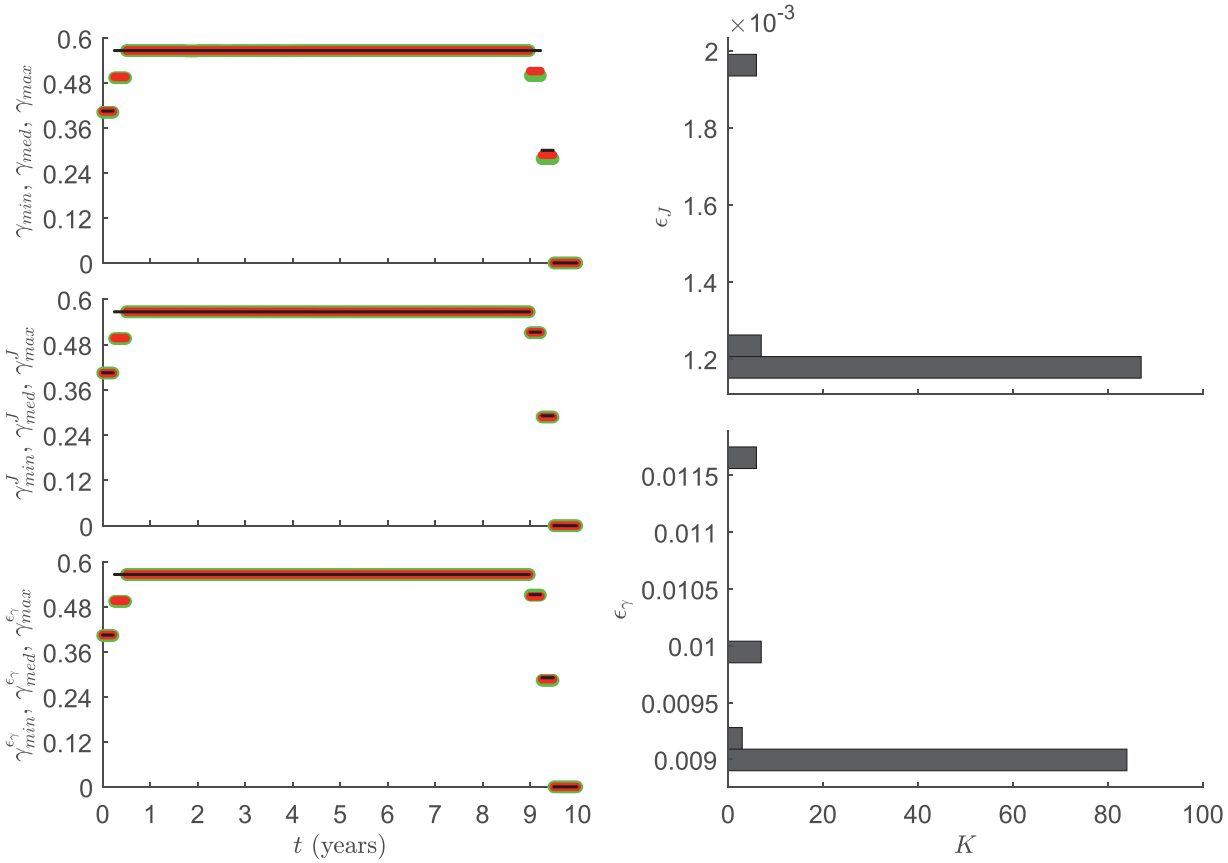

Fig. 6. Statistical assessment for the case $C_\gamma = C_\gamma^{(o)}$ and simulation scenario C5. Data obtained by applying $K = 100$ times the PSO algorithm. Left top panel: $\gamma_{\min}(t)$ (green line), $\gamma_{med}(t)$ (red line) and $\gamma_{\max}(t)$ (black line). Left central panel: $\gamma^J_{\min}(t)$ (green line), $\gamma^J_{med}(t)$ (red line) and $\gamma^J_{\max}(t)$ (black line). Left bottom panel: $\gamma^{\epsilon_\gamma}_{\min}(t)$ (green line), $\gamma^{\epsilon_\gamma}_{med}(t)$ (red line) and $\gamma^{\epsilon_\gamma}_{\max}(t)$ (black line). Right panels: distribution of ϵ_J (top panel) and of ϵ_γ (bottom panel). Parameter values and initial data as in Fig. 3. (For interpretation of the references to colour in this figure legend, the reader is referred to the web version of this article.)

when the deterministic computations converge, the global nature of the resulting optimum can be validated by means of the PSO and DE methods.

To better understand the nature of the non-convergence, we focus on FBS method and plot the values of J_n versus n, where J_n is the value assumed by J (12) at the nth iteration of the algorithm. We notice that in some cases the discrete orbits are periodic (as in the left panels of Fig. 10), in other cases they seem chaotic or at least quasi-periodic (as in the right panel of Fig. 10).

Given an OC problem with finite horizon and upper and lower constant bounds for the control, the FBS algorithm aims at numerically solving the Pontryagin differential-algebraic system characterising the solution of the OC problem:

$$\begin{aligned} \dot{x} &= \partial_\lambda H \\ \dot{\lambda} &= -\partial_x H \\ \partial_u H &= 0 \\ u_{\min} &\le u(t) \le u_{\max} \end{aligned}$$

where H is the Hamiltonian associated to the OC problem to be solved. For the sake of the simplicity, suppose that the above constrained DA equations can be rewritten as follows

$$\begin{aligned} u(t) &= U(x, \lambda) \\ \dot{x} &= F(x, u(t)) \\ \dot{\lambda} &= G(\lambda, x, u(t)). \end{aligned}$$

Then, the FBS algorithm can be summarized as follows. Let $w_n \in \mathbb{R}^q$, $x_n \in \mathbb{R}^l$ and $\lambda_n \in \mathbb{R}^l$ denote the vectors of the discretized approximations of $u(t)$, x and λ in $[0, T]$, respectively, where $q = 40$ and $l = 5000$ in our computations. Let us proceed as follows

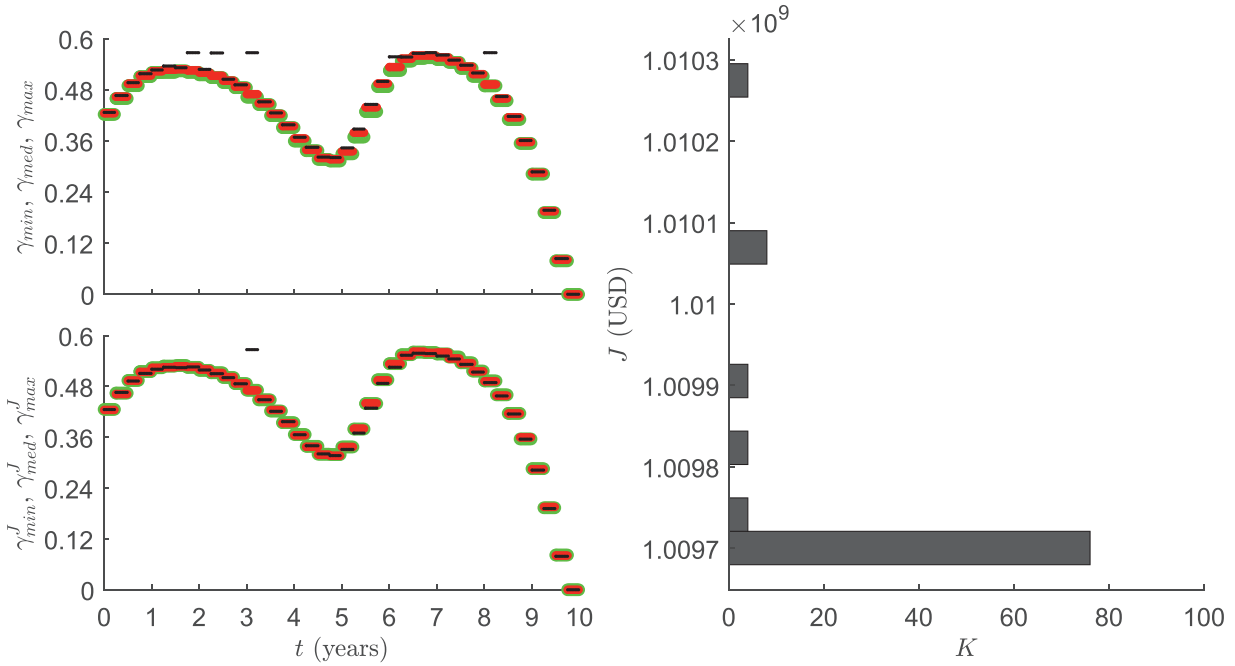

Fig. 7. Statistical assessment for the case $C_\gamma = 5C_\gamma^{(o)}$ with 3 months programming and simulation scenario C1. Data obtained by applying $K = 100$ times the PSO algorithm. Left top panel: $\gamma_{\min}(t)$ (green line), $\gamma_{med}(t)$ (red line) and $\gamma_{\max}(t)$ (black line). Left bottom panel: $\gamma^J_{\min}(t)$ (green line), $\gamma^J_{med}(t)$ (red line) and $\gamma^J_{\max}(t)$ (black line). Right panel: distribution of J. Parameter values and initial data as in Fig. 3. (For interpretation of the references to colour in this figure legend, the reader is referred to the web version of this article.)

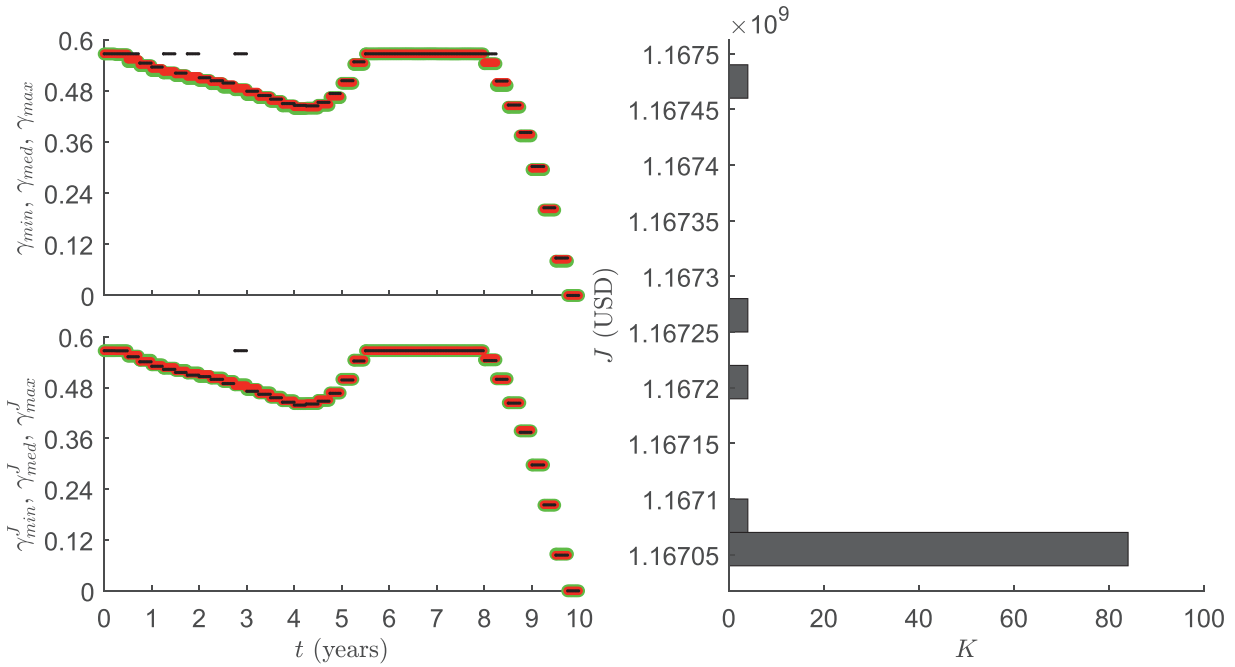

Fig. 8. Statistical assessment for the case $C_\gamma = 5C_\gamma^{(o)}$ with 3 months programming and simulation scenario C3. Data obtained by applying $K = 100$ times the PSO algorithm. Left top panel: $\gamma_{\min}(t)$ (green line), $\gamma_{med}(t)$ (red line) and $\gamma_{\max}(t)$ (black line). Left bottom panel: $\gamma^J_{\min}(t)$ (green line), $\gamma^J_{med}(t)$ (red line) and $\gamma^J_{\max}(t)$ (black line). Right panel: distribution of J. Parameter values and initial data as in Fig. 3. (For interpretation of the references to colour in this figure legend, the reader is referred to the web version of this article.)

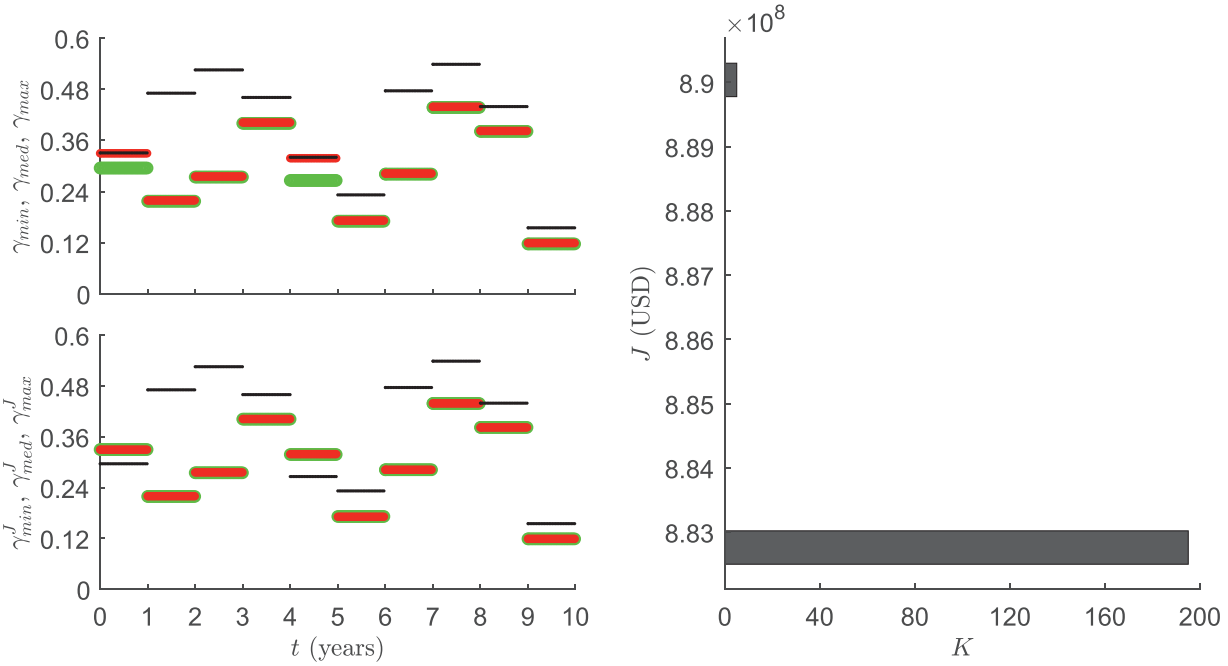

Fig. 9. Statistical assessment for the case $C_\gamma = 5C_\gamma^{(o)}$ with 1 year programming and simulation scenario C5. Data obtained by applying $K = 200$ times the PSO algorithm. Left top panel: $\gamma_{\min}(t)$ (green line), $\gamma_{med}(t)$ (red line) and $\gamma_{\max}(t)$ (black line). Left bottom panel: $\gamma^J_{\min}(t)$ (green line), $\gamma^J_{med}(t)$ (red line) and $\gamma^J_{\max}(t)$ (black line). Right panel: distribution of J. Parameter values and initial data as in Fig. 3. (For interpretation of the references to colour in this figure legend, the reader is referred to the web version of this article.)

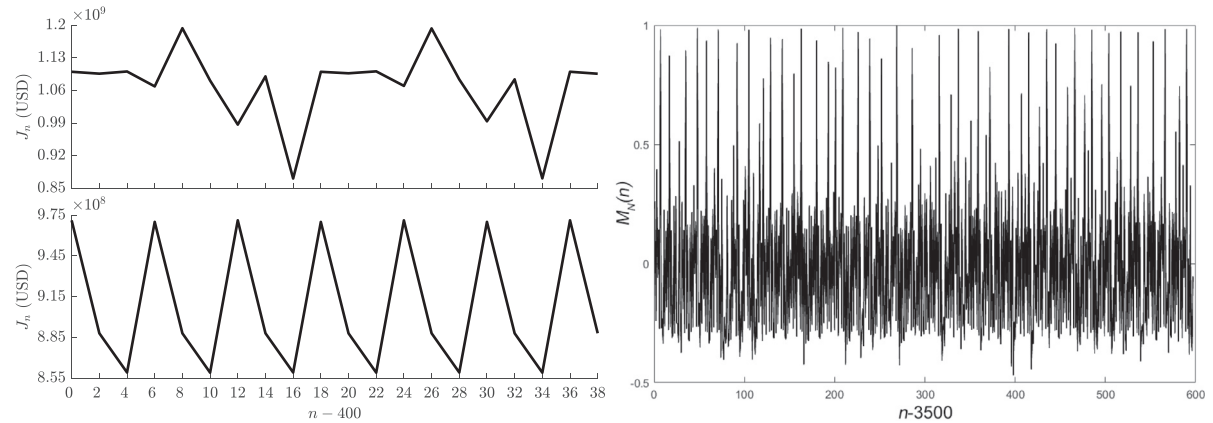

Fig. 10. FBS non-convergence analysis for the case $C_\gamma = 5C_\gamma^{(o)}$ with $\gamma^{(0)}(t) = \gamma_{PSO}(t)$. Left top panel: period 7 orbits of the objective functional J_n in the scenario C1 for $400 \le n \le 438$. Left bottom panel: period 3 orbits of the objective functional J_n in the scenario C4 for $400 \le n \le 438$. Right panel: plot of 600 components of the normalized series M_N (21) of objective functional values in the scenario C5, which exhibits a far more complex pattern than the time-series shown in the other two panels.

- ***Step 0***: w_0 is an initial hint discretized solution;
- ***Step 1***: given w_n, by adopting a Runge–Kutta (RK) algorithm to solve $\dot{x} = F(x, w_n)$, obtain $x_n = f(w_n)$;
- ***Step 2***: given (w_n, x_n), by adopting a RK algorithm to solve $\dot{\lambda} = G(\lambda, x_n, w_n)$, obtain $\lambda_n = g(w_n, x_n)$;
- ***Step 3***: given (w_n, x_n, λ_n), compute $w_{n+1} = (w_n + U(x_n, \lambda_n))/2$;
- ***Step 4***: setting $err \ll 1$, **if**

$$\min(err|w_n| - |w_{n+1} - w_n|, err|x_n| - |x_{n+1} - x_n|, err|\lambda_n| - |\lambda_{n+1} - \lambda_n|) > 0,$$

then STOP, **else** go to Step 1.

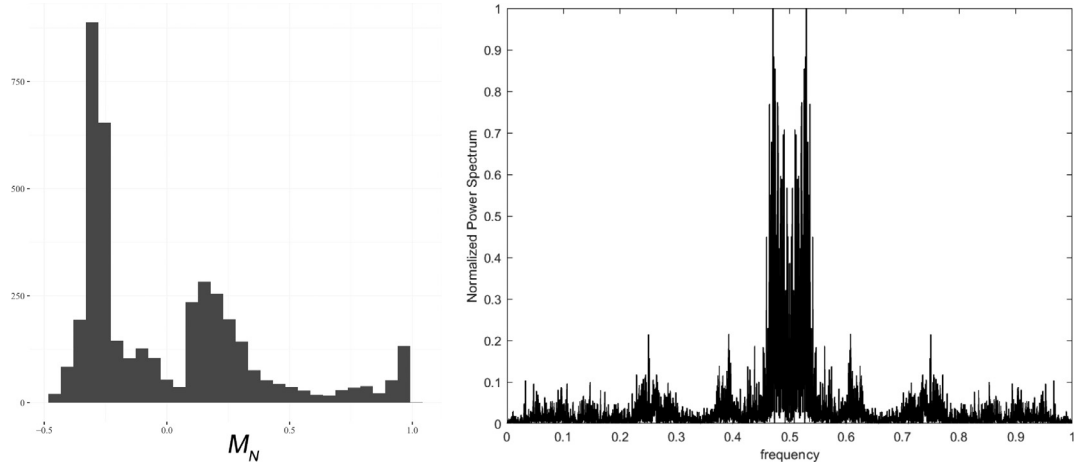

Fig. 11. FBS non-convergence analysis for the case $C_\gamma = 5C_\gamma^{(o)}$ with $\gamma^{(0)}(t) = \gamma_{PSO}(t)$ and simulation scenario C5. The histogram (left panel) and the power spectrum (right panel) of the normalized time-series M_N (21).

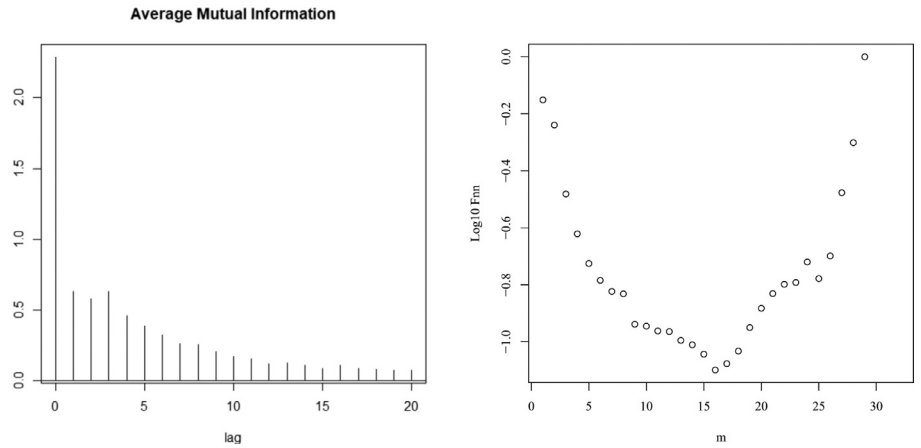

Fig. 12. FBS non-convergence analysis for the case $C_\gamma = 5C_\gamma^{(o)}$ with $\gamma^{(0)}(t) = \gamma_{PSO}(t)$ and simulation scenario C5. Mutual information (left panel) and false nearest neighbors (right panel) plots of the normalized time-series M_N (21).

Importantly, note that the FBS algorithm does not involve the computation of J_n: the stop condition of the ***Step 4*** is *unrelated* to

$$J_n = \omega(w_n),$$

where $\omega(w_n)$ is a suitable discretized approximation of the objective functional $\int_0^T L(x, u(t))dt$. Thus, we add a ***Step 3bis***: compute J_n. In such a way, the out-of transitory 'time'-series

$$M = \{J_n\}_{n=n_1}^{n_f} \tag{20}$$

(in our case: $n_1 = 400$ and $n_f = 4496$) can be analyzed within the well established framework of the statistical theory of nonlinear time-series [25,29,30]. Our analysis is based on the version 13.1 of the *Cran R* library tseriesChaos [16,30].

After normalizing M as follows:

$$M_N = \frac{M - \mu_M}{\sigma_M}, \tag{21}$$

where μ_M and σ_M are the mean and the standard error of M (20), we compute the fast Fourier transform-based power spectrum and the histogram of M_N, see Fig. 11. The histogram reveals a roughly trimodal structure of M_N, where one of its mode is its maximum value. The left part of the (symmetric, of course) power spectrum shows an interval of large peaks for frequencies, namely (0.45,0.5), plus other smaller but appreciable remarkable intervals of peaks distributed on the whole interval (0,0.5).

The mutual information plot [29,30] of M_N (left panel of Fig. 12) has its first relative minimum at a delay $d = 2$, and the false nearest neighbors plot [29,30] for $d = 2$ (right panel of Fig. 12) has its minimum at the embedding dimension $m = 16$.

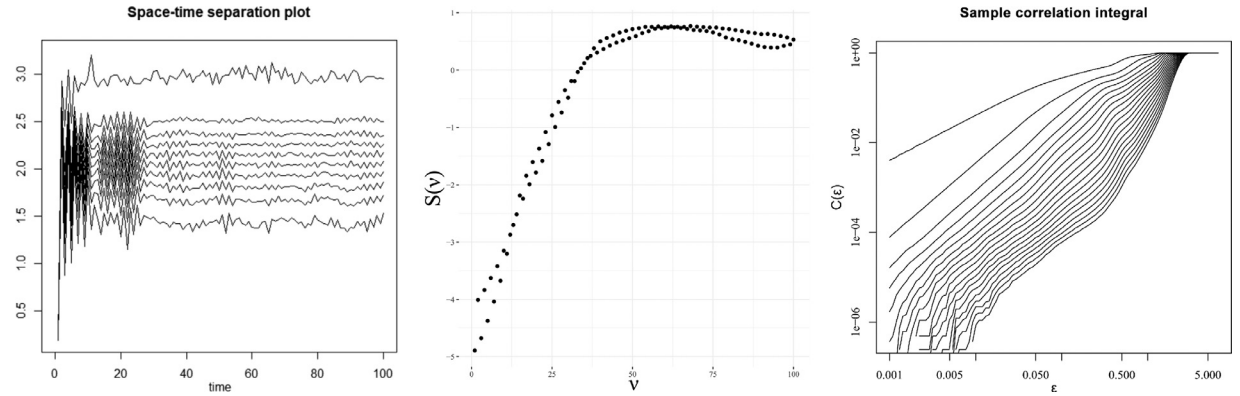

Fig. 13. FBS non-convergence analysis for the case $C_\gamma = 5C_\gamma^{(o)}$ with $\gamma^{(0)}(t) = \gamma_{PSO}(t)$ and simulation scenario C5. Left panel: space-time separation plot to determine the Theiler window to be adopted in the analysis of the time-series M_N (21). Central panel: Lyapunov diagram for the time-series M_N. Right panel: sample correlation integral of the time-series M_N for $2 \leq m \leq 20$.

Virtually, all nonlinear (also even linear) time-series have a larger or smaller 'temporal' correlation structure, which has to be taken into the account in the statistical detection of their chaotic features to avoid wrong results. The space-time separation plot [29,30] of M_N shown in the left panel of Fig. 13 shows that data in M_N have a long correlation to set the Theiler window length [29,30] to $\vartheta = 30$.

Based on the above setting $(\vartheta, d, m) = (30, 2, 16)$, the corresponding Lyapunov diagram [29,30] (see the central panel of Fig. 13) shows a linear structure for $2 \leq \nu \leq 40$, followed by a plateau. By applying a linear statistical model to regress the linear zone of the diagram, we obtain the following estimate of the Lyapunov exponent: $\Lambda = 0.1344 > 0$, with a very small standard error $SE = 0.00368$ with high significance (p-value $< 2 \times 10^{-16}$). This shows that the time-series is chaotic and not quasi-periodic.

The sample correlation integral plot [30] for $2 \leq m \leq 20$ associated to M_N is shown in the right panel of Fig. 13. By applying a linear statistical model to regress the linear zone of the diagram, we obtain the following estimate: for $m = 16$ the estimated correlation dimension is $D_{16} = 1.475912$ with $SE = 0.007433$ (p-value $< 2 \times 10^{-16}$). To compare, for $m = 13$ we estimate $D_{13} = 1.59546$ with $SE = 0.01260$ (p-value $< 2 \times 10^{-16}$).

As shown first by Hurley and Martin [31], recursive algorithms as simple as the Newton methods can exhibit chaotic solutions. Although its principles are simple, FBS is highly dimensional and complex, so that our results suggest that in some cases FBS might have a fractal basin of attraction for its fixed point, so that the choice of the initial hint is more crucial than one could think, and (due to the above-mentioned fractality) the choice of an initial hint leading to the fixed point can sometime become unfeasible. This implies that one should adopt multiple shooting (a very heavy numerical technique, which can also have numerical problems) or direct optimization (as we do, motivated by the nature of the problem in study). In the first case, the complexity and the possible numerical problems due to the frequently stiff nature of the Pontryagin DA equations are an obstacle; in the second case, one rapidly gets the optimal solutions but this is obtained at the price of totally neglecting the important and powerful results of the Pontryagin method. Indeed, direct methods are a sort of black box methods, from the OC theory viewpoint. Apart the above consideration, which could be the cause of the chaoticity in the time-series we analyze? By analogy with the chaos in the Newton method, where chaos occurs in case of multiple fixed points [31], we can hypothesize that the chaoticity we observe could be linked to the presence of multiple local minima of the functional (i.e. of multiple fixed points of the discrete dynamical system induced by the algorithm).

11. Concluding remarks

In modern society dominated by information and noises coming from Internet, especially through social networks such as Facebook, Twitter, Instagram, TikTok, etc., the citizens' opinions are extremely volatile. This makes it appropriate to assume that the time-scales of imitation speed [4,17,18] are nowadays very short. Hence, we apply a quasi-steady-state approximation (QSSA) to the imitation game dynamics equation modelling the vaccine propensity of the target population. On the one hand, of course, the QSSA implies the loss of some information on the dynamics, but, on the other hand, it allows to better understand the mechanisms underlying the nonlinear system to which it is applied, of course in the scenarios it can be applied.

In the case of the model [17], the application of the QSSA shows that the dynamics of the system is ruled by a particular case of 'open-loop' control, where the control, i.e. $\gamma(t)$, impacts in a nonlinear fashion on the controlled system, i.e. the epidemic system. This in turn allows us to determine the conditions for disease elimination through awareness campaigns. Note that in case of low and medium imitation speed, corresponding to classical societies with far less volatile opinion, where the QSSA cannot be applied, the elimination condition and the general behaviour of the system are far more complex and less conclusive [10]. The QSSA also allows us to better explain the classical behavioural SIR model with voluntary

vaccination introduced by d'Onofrio et al. [19]. In particular, the nonzero baseline vaccination rate is related through an increasing function to the actions enacted by the PHS to favour the vaccine uptake.

We then investigate one of most important forms of feedback-based control, of the great relevance in health economy, the optimal control. The resulting optimal control problem presents, w.r.t. the nonlinear 'open-loop' case above commented, a further intriguing feature: the requirements of classical existence theorems are not satisfied. This implies that one has no guarantee that the control obtained with the Pontryagin procedure is a real minimum. We can only suspect that it is a real minimum. As such it requires a double checking.

The two most widespread recursive numerical algorithms to solve the Pontryagin boundary value problem are the FBS and the Grad methods. We apply them to numerically find the optimal control proceeding 'as if' the optimality sufficient conditions hold. The second checking consists in validating the result by applying a direct global optimization by heuristic optimization algorithms: PSO and DE. Furthermore, the use of HOAs is also and mainly needed since for large values of the specific cost of PHS information campaigns (C_γ), the FBS and the Grad algorithms have convergence problems, both by adopting various generic initial hints and by adopting as initial hint the outputs of the HOAs.

We obtain optimal intervention profiles that are strongly oscillating in the scenario where $C_\gamma = 5C_\gamma^{(0)}$, being $C_\gamma^{(0)}$ the baseline value. The obtained optimal controls are qualitatively similar to those obtained in the case of slow imitation speed and reported in [12]. However, in the fast system the solutions found by the PSO algorithm are more smooth and quantitatively different. We also consider alternative schedules with less frequent update of the strategy: namely we investigate the cases where the strategy is only yearly updated and the extreme case where it is biennially updated. In both cases the non-monotone nature of the control is maintained. In all cases we consider, the solutions obtained by the DE algorithm, which are (roughly speaking) 'quite noisy', show that the system is robust to multiple local deviations from the theoretical optimum: this robustness is of interest since in real world maintaining a strict scheduling can be difficult.

PSO and DE are stochastic algorithms, i.e. they transform the initial time-continuous dynamical system in a discrete-time stochastic dynamical system. On the one hand, stochasticity is fundamental to find the global optimum and not to be stuck in a local minimum, on the other hand this implies that the output of a single run of an HOA is an instance from a probabilistic distribution, which in our case is multivariate in a large dimension space. For this reason, we propose in this work to couple the use of HOAs in OC problems with a double statistical assessment: (i) of the time profile of the control $\gamma(t)$; (ii) of the value of the objective functional J. This will provide the system designers (in our case the PHS officers) an interesting tool to assess the robustness of the optimal control strategy. Namely in our case, although the sample size is relatively small due to constraints on the available computational resources, the statistical assessment suggests that the PSO algorithm for the problem in study finds the actual global minimum.

Lastly, stimulated by the non-convergence of the indirect optimization methods, we decide to investigate the nature of this non-convergence, by focusing on the FBS method case. In the problem in study, we analyze the 'time'-series J_n (where the 'time' n is the iteration number) of the objective functional and we obtain that: (i) in some cases the time-series is attracted by a periodic attractor, of period > 2; (ii) in other cases the time-series are more complex and highly erratic. We apply methods of nonlinear time-series theory [16,25,29,30] to explore the features of the latter series. We obtain that they are chaotic.

11.1. Future perspectives

Apart the very basic nature of the SIR model, the major limit of our results is that the system to be controlled is deterministic and that the control is purely deterministic as well. However, we note that the heuristic procedures we illustrate here can be applied to stochastic versions of our OC problem. Namely, we plan to investigate a stochastic OC problem based on our model where the following stochastic fluctuations are included: (i) stochastic demographic and epidemic fluctuations modelled by the so-called chemical Langevin equation approach [26]; (ii) stochastic fluctuations of the contact rate.

Another line of research we will soon approach remains, instead, in the deterministic path: application of the investigation we propose here to the Bauch behavioural epidemic model [4], which has a number of features that makes it quite distinct from the problem we face here.

Finally, we are also designing a new behavioural epidemic model, where the possibility of vaccination (so far limited at newborns) is extended at all ages. All ages vaccination is particularly relevant for emergent and re-emergent diseases. In such a case, the modelling process involves two critical issues to face: the first one is that not only parents but all individuals are subject to the game-theoretical mechanisms between pro and anti-vaccine forces; the second one is the possibility that disease natural or vaccine-induced immunity is not long-lasting – as for childhood diseases –, but time-vanishing (as typical, for example, of seasonal flu vaccines).

Declaration of Competing Interest

The authors declare that they have no known competing financial interests or personal relationships that could have appeared to influence the work reported in this paper.

CRediT authorship contribution statement

Rossella Della Marca: Data curation, Investigation, Software, Validation, Visualization, Writing - original draft. **Alberto d'Onofrio:** Conceptualization, Data curation, Formal analysis, Investigation, Methodology, Supervision, Validation, Visualization, Writing - original draft.

Acknowledgements

We are thankful to the anonymous reviewers for their constructive comments, which have improved the earlier version of the manuscript. We gratefully acknowledge the financial support of the LIS LYSM AMU-CNRS-ECM-INdAM, which allowed a two-months scientific visit of RDM at the International Prevention Research Institute in Lyon, France. This research benefited from the HPC (High Performance Computing) facility of the University of Parma, Italy. The work was also performed in the frame of the activities sponsored by INdAM-GNFM.

Appendix A. Asymptotic behaviour in case of periodic $\gamma(t)$

From the differential inequality

$$\dot{S} \le \mu(1 - \zeta(0, \gamma(t)) - S)$$

it follows that $S \le Y$, where Y is given by

$$\dot{Y} = \mu(1 - \zeta(0, \gamma(t)) - Y), \tag{22}$$

with $Y(0) = S(0)$. Note that asymptotically the solution of (22) is periodic, and we denote it as $Y_\infty(t)$. Moreover, from

$$\dot{I} \le I(\beta Y - \nu - \mu) = (\nu + \mu) I(\mathcal{R}_0 Y - 1)$$

it straightforwardly follows that if

$$\mathcal{R}_0 \frac{1}{T} \int_0^T Y_\infty(t) dt < 1, \tag{23}$$

then $I \to 0$ and, as a consequence, $\dot{S} \to \mu(1 - \zeta(0, \gamma(t)) - S)$, yielding in turn that $S(t) \to Y_\infty(t)$. In other words, (S, I) tends to the disease-free solution

$$(Y_\infty(t), 0). \tag{24}$$

Since $Y_\infty(t)$ solves (22), by integrating over a period $[0, T]$, we get

$$\frac{1}{T} \int_0^T Y_\infty(t) dt = 1 - \frac{1}{T} \int_0^T \zeta(0, \gamma(t)) dt - \frac{1}{\mu T} \int_0^T \dot{Y}_\infty(t) dt = 1 - \frac{1}{T} \int_0^T \zeta(0, \gamma(t)) dt.$$

Thus, condition (23) becomes

$$\mathcal{R}_0 \left(1 - \frac{1}{T} \int_0^T \zeta(0, \gamma(t)) dt \right) < 1.$$

Linearising at the disease-free solution (24), one gets

$$\dot{i} = i(\beta Y_\infty(t) - \nu - \mu).$$

As a consequence, if

$$\mathcal{R}_0 \left(1 - \frac{1}{T} \int_0^T \zeta(0, \gamma(t)) dt \right) > 1,$$

then the disease-free solution is unstable.

Appendix B. Explicit solution of equation (18)

Eq. (18) can be obtained from the general cubic equation

$$a_1 z^3 + a_2 z^2 + a_3 = 0, \tag{25}$$

by substituting $z = \gamma(t)$, $a_1 = 4\alpha$, $a_2 = \theta^2(I)$, and $a_3 = -(\lambda_1 \mu - C_\nu)^2 / (4C_\gamma^2)$.

Let us introduce the quantities

$$P = -\frac{a_2^2}{9a_1^2}, \; Q = \frac{2a_2^3 + 27a_1^2 a_3}{27a_1^3}$$

and the discriminant $\Delta = 4P^3 + Q^2$. Then, the solutions of (25) are [37]

$$\begin{aligned} z_1 &= \sqrt[3]{\frac{-Q+\sqrt{\Delta}}{2}} + \sqrt[3]{\frac{-Q-\sqrt{\Delta}}{2}}, \\ z_2 &= e^{\frac{2\pi i}{3}} \sqrt[3]{\frac{-Q+\sqrt{\Delta}}{2}} + e^{\frac{4\pi i}{3}} \sqrt[3]{\frac{-Q-\sqrt{\Delta}}{2}}, \\ z_3 &= e^{\frac{4\pi i}{3}} \sqrt[3]{\frac{-Q+\sqrt{\Delta}}{2}} + e^{\frac{2\pi i}{3}} \sqrt[3]{\frac{-Q-\sqrt{\Delta}}{2}}. \end{aligned} \tag{26}$$

Being $a_1 > 0$, $a_2 > 0$, $a_3 < 0$, from Descartes' rule of signs it follows that one of the roots (26) is real and positive, whilst the other two have negative real part. Specifically, the latter are real [resp. complex conjugates] if $\Delta \leq 0$ [resp. $\Delta > 0$].

Funding. This research did not receive any specific grant from funding agencies in the public, commercial, or not-for-profit sectors.

Supplementary material

Supplementary material associated with this article can be found, in the online version, at 10.1016/j.cnsns.2021.105768

References

[1] Alberici AI, Milesi P. The influence of the internet on the psychosocial predictors of collective action. J Commun Appl Soc Psychol 2013;23(5):373–88.
[2] Aniţa S, Capasso V, Arnăutu V. An introduction to optimal control problems in life sciences and economics. New York: Birkhäuser/Springer; 2011.
[3] Arnăutu V, Barbu V, Capasso V. Controlling the spread of a class of epidemics. Appl Math Optim 1989;20(1):297–317.
[4] Bauch CT. Imitation dynamics predict vaccinating behaviour. Proc R Soc Ser B 2005;272(1573):1669–75.
[5] Bolzoni L, Bonacini E, Della Marca R, Groppi M. Optimal control of epidemic size and duration with limited resources. Math Biosci 2019;315:108232.
[6] Bowong S, Aziz Alaoui AM. Optimal intervention strategies for tuberculosis. Commun Nonlinear Sci Numer Simul 2013;18(6):1441–53. doi:10.1016/j.cnsns.2012.08.001. http://www.sciencedirect.com/science/article/pii/S1007570412003437
[7] Bozorg-Haddad O, Solgi M, Loaiciga HA. Meta-heuristic and evolutionary algorithms for engineering optimization, 294. Hoboken: John Wiley & Sons; 2017.
[8] Broniatowski DA, Jamison AM, Qi S, AlKulaib L, Chen T, Benton A, et al. Weaponized health communication: Twitter Bots and Russian trolls amplify the vaccine debate. Am J Public Health 2018;108(10):1378–84.
[9] Buonomo B, Carbone G, d'Onofrio A. Effect of seasonality on the dynamics of an imitation-based vaccination model with public health intervention. Math Biosci Eng 2018;15(1):299–321.
[10] Buonomo B, Chitnis N, d'Onofrio A. Time heterogeneous programs of vaccination awareness: modeling and analysis. Ric Mat 2018;67(1):205–25.
[11] Buonomo B, Della Marca R, d'Onofrio A. Optimal public health intervention in a behavioural vaccination model: the interplay between seasonality, behaviour and latency period. Math Med Biol: A Journal of the IMA 2018;36(3):297–324. doi:10.1093/imammb/dqy011. https://academic.oup.com/imammb/article-pdf/36/3/297/29963443/dqy011.pdf
[12] Buonomo B, Manfredi P, d'Onofrio A. Optimal time-profiles of public health intervention to shape voluntary vaccination for childhood diseases. J Math Biol 2019;78(4):1089–113.
[13] Chen S, Montgomery J, Bolufé-Röhler A. Measuring the curse of dimensionality and its effects on particle swarm optimization and differential evolution. Appl Intell 2015;42(3):514–26.
[14] Cosentino C, Bates D. Feedback control in systems biology. Boca Raton: Crc Press; 2011.
[15] Das S, Abraham A, Konar A. Particle swarm optimization and differential evolution algorithms: technical analysis, applications and hybridization perspectives. In: Liu Y, Sun A, Loh HT, Lu WF, Lim EP, editors. Advances of computational intelligence in industrial systems. Berlin, Heidelberg: Springer; 2008. p. 1–38.
[16] Di Narzo A.F.. tseriesChaos: Analysis of Nonlinear Time Series; 2019. R package version 13.1; https://cran.r-project.org/web/packages/tseriesChaos/a.a
[17] d'Onofrio A, Manfredi P, Poletti P. The impact of vaccine side effects on the natural history of immunization programmes: an imitation-game approach. J Theor Biol 2011;273(1):63–71.
[18] d'Onofrio A, Manfredi P, Poletti P. The interplay of public intervention and private choices in determining the outcome of vaccination programmes. PLoS One 2012;7(10):e45653.
[19] d'Onofrio A, Manfredi P, Salinelli E. Vaccinating behaviour, information, and the dynamics of SIR vaccine preventable diseases. Theor Popul Biol 2007;71(3):301–17.
[20] Elnagar G, Kazemi MA, Razzaghi M. The pseudospectral Legendre method for discretizing optimal control problems. IEEE Trans Autom Control 1995;40(10):1793–6.
[21] Fleming WH, Rishel RW. Deterministic and stochastic optimal control. Applications of Mathematics, 1. Berlin, New York: Springer; 1975.
[22] Frey E. Evolutionary game theory: theoretical concepts and applications to microbial communities. Phys A 2010;389(20):4265–98.
[23] Garg D, Patterson M, Hager WW, Rao AV, Benson DA, Huntington GT. A unified framework for the numerical solution of optimal control problems using pseudospectral methods. Automatica 2010;46(11):1843–51.
[24] Gersovitz M, Hammer JS. The economical control of infectious diseases. Econ J 2003;114(492):1–27.
[25] Giannerini S. 3 - the quest for nonlinearity in time series. In: Subba Rao T, Subba Rao S, Rao CR, editors. Time series analysis: methods and applications. Handbook of Statistics, 30. Elsevier; 2012. p. 43–63. doi:10.1016/B978-0-444-53858-1.00003-X.
[26] Gillespie DT. The chemical Langevin equation. J Chem Phys 2000;113(1):297–306.
[27] Glauber RJ. Time-dependent statistics of the Ising model. J Math Phys 1963;4(2):294–307.
[28] Goto N, Kawable H. Direct optimization methods applied to a nonlinear optimal control problem. Math Comput Simul 2000;51(6):557–77.
[29] Hegger R, Kantz H, Schreiber T. Practical implementation of nonlinear time series methods: the TISEAN package. Chaos 1999;9(2):413–35.
[30] Huffaker R, Bittelli M, Rosa R. Nonlinear time series analysis with R. Oxford: Oxford University Press; 2017.
[31] Hurley M, Martin C. Newton's algorithm and chaotic dynamical systems. SIAM J Math Anal 1984;15(2):238–52.
[32] Jang J, Kwon H-D, Lee J. Optimal control problem of an SIR reaction-diffusion model with inequality constraints. Math Comput Simul 2020;171:136–51.
[33] Jost JT, Barber P, Bonneau R, Langer M, Metzger M, Nagler J, et al. How social media facilitates political protest: information, motivation, and social networks. Adv Polit Psychol 2018;39(S1):85–118. doi:10.1111/pops.12478.
[34] Kamens DH. Chapter 9 The construction of public opinion. In: Kamens DH, editor. Beyond the nation-state. Bingley: Emerald Group Publishing Limited; 2012. p. 257–79.
[35] Kennedy J, Eberhart R. Particle swarm optimization. In: Proceedings of the IEEE international conference on neural networks, Perth, Australia; 1995. p. 1942–5.
[36] Kirk DE. Optimal control theory: an introduction. New Jersey: Prentice–Hall; 1970.

[37] Kurosh AG. Higher algebra. Moscow: Mir Publishers; 1972.
[38] Lemos-Paião AP, Silva CJ, Torres DFM, Venturino E. Optimal control of aquatic diseases: a case study of Yemen's cholera outbreak. J Optim Theory Appl 2020:1–23.
[39] Lenhart S, Workman JT. Optimal control applied to biological models. London: Crc Press; 2007.
[40] Lin C-C, Segel LA. Mathematics applied to deterministic problems in the natural sciences. Philadelphia: SIAM; 1988.
[41] Machado JAT, Abedi Pahnehkolaei SM, Alfi A. Complex-order particle swarm optimization. Commun Nonlinear Sci Numer Simul 2021;92:105448. doi:10.1016/j.cnsns.2020.105448. http://www.sciencedirect.com/science/article/pii/S1007570420302781
[42] Modeling the interplay between human behavior and the spread of infectious diseases. Manfredi P, d'Onofrio A, editors. New York: Springer; 2013.
[43] Marquez HJ. Nonlinear control systems: analysis and design. Hoboken: John Wiley & Sons; 2003.
[44] MATLAB. Matlab release 2019b. The MathWorks, Inc., Natick, MA. 2019.
[45] McAsey M, Mou L, Han W. Convergence of the forward-backward sweep method in optimal control. Comput Optim Appl 2012;53(1):207–26.
[46] Mezura-Montes E, Coello CAC. Constraint-handling in nature-inspired numerical optimization: Past, present and future. Swarm Evol Comput 2011;1(4):173–94. doi:10.1016/j.swevo.2011.10.001. http://www.sciencedirect.com/science/article/pii/S2210650211000538
[47] On J, Park H-A, Song T-M. Sentiment analysis of social media on childhood vaccination: development of an ontology. J Med Internet Res 2019;21(6):e13456. doi:10.2196/13456.
[48] Osborne MR. On shooting methods for boundary value problems. J Math Anal Appl 1969;27(2):417–33.
[49] Pedersen MEH. Good parameters for particle swarm optimization. Tech. Rep.. Copenhagen, Denmark: Hvass Laboratories; 2010.
[50] Pontryagin LS, Boltyanskii VG, Gamkrelidze RV, Mishenko EF. The mathematical theory of optimal processes. New York: John Wiley & Sons; 1962.
[51] Price K., Storn R.M.. Differential evolution (DE) for continuous function optimization. http://www1.icsi.berkeley.edu/~storn/code.html; (Accessed on September 2020).
[52] Price K, Storn RM, Lampinen JA. Differential evolution: a practical approach to global optimization. Berlin, Heidelberg: Springer; 2006.
[53] Schättler H, Ledzewicz U. Geometric optimal control: theory, methods and examples. Interdisciplinary Applied Mathematics, 38. New York: Springer; 2012.
[54] Sharomi O, Malik T. Optimal control in epidemiology. Ann Oper Res 2017;251(1-2):55–71.
[55] Silva CJ, Maurer H, Torres DFM. Optimal control of a tuberculosis model with state and control delays. Math Biosci Eng 2017;14(1):321–37. doi:10.3934/mbe.2017021. http://aimsciences.org//article/id/b0c9f6b6-2979-418c-b88c-df7ba6147cb4
[56] Storn R. On the usage of differential evolution for function optimization. In: Proceedings of North American fuzzy information processing. IEEE; 1996. p. 519–23.
[57] Storn R, Price K. Differential evolution—A simple and efficient heuristic for global optimization over continuous spaces. J Glob Optim 1997;11(4):341–59.
[58] Tikhonov AN. Systems of differential equations containing small parameters in the derivatives. Mat Sb 1952;73(3):575–86.
[59] Verhulst F. Singular perturbation methods for slow-fast dynamics. Nonlinear Dyn 2007;50(4):747–53.
[60] Vesterstrøm J, Thomsen R. A comparative study of differential evolution, particle swarm optimization, and evolutionary algorithms on numerical benchmark problems. In: Proceedings of the 2004 congress on evolutionary computation (IEEE Cat. No.04TH8753), 2; 2004. p. 1980–7.
[61] von Stryk O. Numerical solution of optimal control problems by direct collocation. In: Bulirsch R, Miele A, Stoer J, K W, editors. Optimal control. Basel: Springer; 1993. p. 129–43.
[62] Wang Z, Bauch CT, Bhattacharyya S, d'Onofrio A, Manfredi P, Perc M, et al. Statistical physics of vaccination. Phys Rep 2016;664:1–113.